NewFields

Character and Sedimentation Rate of "Lingering" Macondo Oil in the Deep-Sea up to One Year after the Deepwater Horizon Oil Spill

Scott A. Stout[1] and Uta Passow[2]

[1]NewFields Environmental Forensics Practice, LLC, Rockland, MA
[2]Marine Science Institute, University of California Santa Barbara, CA
August 2015

Summary

Nineteen sediment trap samples collected over 21-day intervals from a trap located ~6.5 km southwest of the *Deepwater Horizon* oil spill site between ~6 weeks and 14 months after the failed Macondo well was shut-in July 15, 2010 (i.e., late August 2010 to September 2011) were chemically analyzed. The objective was to better understand the deposition of oil-bearing particles that accumulated on the seafloor, i.e., the so-called "*marine oil snow sedimentation and flocculent accumulation*", or MOSSFA event, caused by the *Deepwater Horizon* oil spill. The following conclusions were reached:

- Declining temporal trends in concentrations and sedimentation rates of TPH, PAHs, and biomarkers in the trap samples, as well as their chemical fingerprints indicate increasingly weathered Macondo oil was settling through the water column through August 2011, i.e. more than 1 year after the end of the spill. The lack of evidence for evaporation and photo-oxidation (that would have occurred had the oil formerly reached the sea surface) suggest the oil arriving at the trap was derived mostly (perhaps exclusively) from the deep-sea plume (rather than from sinking surface oil).
- Following the maximal sedimentation of oil in the first trap sample studied (late August 2010) the concentrations and sedimentation rates of Macondo oil gradually decreased over time with increased "pulses" of oil deposition occurring in December 2010 and March/April 2011. A fourth, albeit minor, "pulse" of oil sedimentation occurred in June 2011.
- The overall declining hydrocarbon concentrations and sedimentation rates, progression in weathering of the sinking oil over time, and its overall consistency with the weathered oil residues found on the seafloor following the *Deepwater Horizon* oil spill, indicates the sinking oil was derived from the spill – and not from other sources such as naturally occurring seeps.
- The overall decline in Macondo oil sedimentation rates during the sampling period is attributed to natural dispersion of the vestiges of the deep-sea plume, whereas the distinct "pulses" observed co-occur with increased amounts of sinking particles, that included both organic (diatoms and other plankton) and lithogenic particles that, we contend, scavenged the gradually decreasing amounts of "lingering" oil within the water column for up to about 1 year after the spill ended (i.e. through August 2011).
- Several lines of evidence imply that the vast majority of the material collected in the sediment trap originated from the water column rather than stemming from resuspension from the seafloor below the trap.
- One difference between the Macondo oil in the trap samples and the Macondo oil on the seafloor is the relative higher depletion of triaromatic steroids (TAS) in the former. This difference is hypothesized to have been caused by the greater biodegradation or dissolution of these aromatic biomarkers experienced by the "lingering" oil during its longer residence within the water column, versus the lesser biodegradation or dissolution expressed by the oil on the seafloor following the spill,

which was mostly deposited rapidly and earlier in the spill (i.e., prior to the earliest trap sample studied herein, or pre-late August 2010; see below).

- Sinking particles from the last trap sample collected (Sept. 2011) contained only pyrogenic PAHs, biogenic perylene, and traces of biomarkers, which are believed to represent normal "background" deposition for the area.
- The first trap sample collected (late August 2010) contained an "excess" of 16 Priority Pollutant (unsubstituted) PAHs and had a TPAH16 sedimentation rate that was 20-times higher than existed one year later. The high TPAH16 sedimentation rate (0.62 $\mu g/m^2$/day) in late August 2010 is attributed to settling of pyrogenic PAH-rich combustion residues generated during the *in situ* burning conducted in response to the spill.
- The sedimentation rates calculated for TPH (1,146 $\mu g/m^2$/day), TPAH50 (3.0 $\mu g/m^2$/day), and hopane (0.32 $\mu g/m^2$/day) were highest during the trap's first sampling interval in late August 2010 and declined thereafter. The sedimentation rates prior to this time, i.e., during the active spill, were undoubtedly higher (see next bullet).
- The sedimentation rates for hopane (a conservative marker for the oil) were used to estimate ~ 3.7 barrels (bbl) of Macondo oil were deposited in the km^2 beneath the trap between late August 2010 through August 2011. The concentration of Macondo-derived hopane found in surface (0-1 cm) sediments below the trap – as calculated in another study (Stout et al., 2015) – indicated that the total Macondo oil deposited beneath the trap was on the order of 104 ± 69 bbl/km^2. This large disparity, on average, suggests that only ~3% (3.7 out of 104 bbl) of the Macondo oil on the seafloor ~6.5 km southwest of the well was deposited *after* late August 2010 (when the trap sampling started). Oppositely, this indicates ~97% of the Macondo oil deposited on the seafloor in this area was deposited before late August 2010, i.e., during and immediately after the active oil spill.
- Assuming the trap's location largely is representative of the deep-sea, the vast majority of the Macondo oil found on the seafloor in 2011 was deposited before late August 2010, i.e., during the main MOSSFA "dirty blizzard(s)". After the "blizzard(s)", increasingly less "lingering" oil remained in (and was scavenged from) the water column through August 2011.

Introduction

Marine snow, defined as composite particles > 0.5 mm in size, is a natural and ubiquitous phenomenon in oceans wherein aggregates of inorganic (e.g., litho- and biogenic minerals) and/or organic particles (e.g., phytoplankton, microbial mucus-rich flocs, zooplankton feces, feeding structures, detritus, or combustion-derived particles) sink sufficiently fast to avoid complete degradation and are eventually deposited on the seafloor (e.g., Alldredge and Silver, 1988). Marine snow is thought to have played an important role in transporting oil from the *Deepwater Horizon* oil spill to the seafloor.

In May and June 2010, in the midst of the *Deepwater Horizon* oil spill, bacteria-mediated, mucus-rich marine snow was observed in surface waters associated with floating oil slicks and sheens from the spill. Visual observations and laboratory studies have shown that the marine snow, or at least some portion of it, eventually lost buoyancy and sank, taking some weathered oil from the sea surface with it to the seafloor (Passow et al. 2012; Passow 2014). Direct evidence for this "marine oil snow" phenomenon was obtained in sediment trap samples collected during the active spill from a sediment trap located 58 km northeast of the well (VK826; Stout and German, 2015). At this location,

oil from the surface (as evidenced by features consistent with photo-oxidation) was observed within days of the spill's beginning, continued throughout the duration of the spill, and then rapidly declined to pre-spill conditions within a few weeks of the spill's end. In this shelf edge location, results showed that Macondo oil formerly at the surface was subsequently deposited on the seafloor during the active spill at a concentration of about 10 barrels (bbl) per km^2.

In addition, oil within the deep-sea plume that had formed (Diercks et al., 2010), i.e., oil that had never reached the sea surface, is also envisioned to have been deposited on the seafloor. The deep-sea plume consisted of both dissolved oil and (neutrally-buoyant) oil droplets, micelles, or particles (reportedly < 100 mm; North et al., 2011) that existed between ~1000 and 1300 m in depth and advected horizontally (mostly) to the southwest from the wellhead (Camilli et al., 2010; Hazen et al., 2010; NOAA 2011; Sokolofsky et al., 2011; Atlas and Hazen, 2011; Ryerson et al., 2012). Marine snow was also observed within the deep-sea plume in May and June 2010 (J. Payne, personal communication)[1] and is believed to have carried oil particles "scavenged" from the deep-sea plume to the seafloor.

The sinking of marine oil snow from the sea surface and deep-sea plume to the seafloor led to the widespread accumulation of oil-bearing "floc" on the seafloor, a phenomenon that has been referred to as "*marine oil snow sedimentation and flocculent accumulation*" or MOSSFA (Kinner et al. 2014). The sediment trap data from the shelf edge confirmed the settling of marine oil snow and projected this phenomenon to have occurred over a large area (~7,600 km^2; Stout and German, 2015). Chemical evidence for the MOSSFA phenomenon and the widespread occurrence of seafloor floc containing Macondo oil has also been obtained from the study of deep-sea sediments (Valentine et al., 2014, Chanton et al., 2015; Romero et al., 2015; Stout, 2015e), deep-sea corals (White et al., 2012; Hsing et al., 2013; Fisher et al., 2014; Brooks et al., 2015), and benthic infauna (Montagna et al., 2013).

Although the formation and sinking marine oil snow and resulting accumulation of seafloor floc containing Macondo oil are unequivocal, questions remain regarding the timing, sedimentation rate (flux), duration, and pathways by which the oily floc was deposited. For example, when and for how long after the spill was the oil-bearing floc deposited on the seafloor? Did the oil within the floc come mainly from oil sinking from the sea surface or from oil present within the deep-sea plume?

In this study, the character, flux, and duration of oil in sinking particles collected from a sediment trap located ~6.5 km southwest of the Macondo wellhead at a water depth of 1,400 m are reported. Twenty (20) trap samples were collected on 21-day intervals spanning from ~6 weeks to 14 months after the failed Macondo well was shut-in July 15, 2010.

The results of this study provide direct evidence that marine oil snow was still settling through the water column at this location through August 2011, i.e. more than 1 year after the end of the spill. The presence of oil in the water column many months after the end of the spill, provides an explanation for the presence of oil in mesozooplankton in the fall of 2010 (Mitra et al. 2012). The sedimentation rate of oil as measured by the trap is much lower than was calculated for the underlying surface sediments from the same area (Stout et al., 2015), suggesting that the vast majority of the oil deposited on

[1] For example, see video from the Jack Fitz 3 NRDA cruise (June 2010) showing occurrence settling behavior of oil particles, marine snow, and mucus strings at depths within the deep-sea plume (Video Files: P6130729.AVI, P6130730.AVI, P6191861.AVI; NOAA DIVER).

the seafloor in this area was deposited prior to late August 2010, when the first trap samples were collected. From this we infer that the oil captured in our trap samples represented only "lingering" vestiges of oil formerly present in the deep-sea plume that had existed during the active spill.

Samples and Methods

Nineteen (19) sediment trap samples were provided to NOAA for analysis by Dr. Uta Passow (University of California, Santa Barbara; Table 1), the amount of material collected in the last, the 20th cup, was not sufficient for detailed analysis. The samples were collected with a Kiel sediment trap (KUM) that was deployed at 28° 42.360'N; 88° 25.325'W, approximately 6.5 km (4 mi) southwest of the Macondo well and 1.6 km east of Biloxi Dome (Figure 1). The water depth at this location was 1,538 m and the trap was set about 105 m above the seafloor, i.e., water depth of about 1,433 m. Thus, the trap depth was below the "floor" of the deep-sea plume (~1,000-1300 m).

Sample bottles (300 mL polypropylene) on a carousel below the funnel-shaped trap (collection surface 0.5 m^2; Fig. 1) collected samples over 21-day intervals starting August 25, 2010 and ending September 28, 2011 (Table 1). Bottle contents were preserved *in situ* during collection with $HgCl_2$ and upon retrieval were maintained cold (4°C) and dark until processed for analysis. Splits (1/8th or 1/16th) of the total particulates collected in each bottle were provided to Alpha Laboratory (Mansfield, MA) for chemical analysis. These samples consisted of artificial seawater slurries, which were transferred to pre-weighed 250 mL glass extraction jars and centrifuged in order to concentrate the collected material.[2] The water was decanted and archived. The concentrated material was split with an aliquot used for dry weight determination (Table 1) and the remainder used for chemical analysis. Because Alpha received 1/8th or 1/16th aliquots of the total sample, the total mass (dry weight) of trap material collected in each sample could be calculated (Table 1). These ranged from 19.3 g (Cup 1) to 2.8 g (Cup 5; Table 1).

The trap samples for chemical analysis were spiked with recovery surrogates and serially-extracted (3x) using fresh dichloromethane (DCM). Each sample's serial extracts were combined, dried with sodium sulfate, and concentrated. The concentrated extracts were then processed through silica gel, eluting with DCM, following adaptations of EPA Method 3630. The silica-cleaned extracts were then concentrated and spiked with internal standards prior to instrument analysis. The extracts were analyzed in accordance with NOAA (2014) for:

(1) *Total Petroleum Material (TPH) and Saturated Hydrocarbon (SHC) Quantification and Fingerprinting*: a modified EPA Method 8015B was used to determine the TPH concentration (C_9-C_{44}) and concentrations of individual *n*-alkanes (C_9-C_{40}) and (C_{15}-C_{20}) acyclic isoprenoids via gas chromatography-flame ionization detection (GC/FID). Concentrations of target compounds are reported in $\mu g/g_{dry}$ (ppm).

[2] The original sample bottles (300 mL polypropylene) were subsequently provided for chemical analysis. This was done as a means to assure that no residual oil was left coating/staining the inside of the jars; subsequent analysis of the jars confirmed the staining observed on the empty polypropylene bottles was not oil. No further analysis was conducted on the original sample bottles.

(2) *PAH, Alkylated PAH and Petroleum Biomarkers:* a modified EPA Method 8270 was used to determine the concentration of (1) approximately 80 PAH, alkylated PAH homologues, individual PAH isomers, and sulfur-containing aromatics and (2) approximately 50 tricyclic and pentacyclic triterpanes, regular and rearranged steranes, and triaromatic steroids via GC/MS operated in the selected ion monitoring mode (SIM). Concentrations of target compounds are reported in $\mu g/g_{dry}$ (ppm). The target analytes for this analysis are listed in Table 2. Note that two PAH totals are given, viz. TPAH16 and TPAH50. TPAH16 represents the total of 16 Priority Pollutant PAH analytes (see bold; Table 2) and TPAH50 represents the total of all 2- to 6-ring PAH analytes ranging from naphthalene to benzo(*g,h,i*)perylene, excluding perylene.

The TPH, SHC, PAH and biomarker concentration data reported herein are non-surrogate corrected. The analytical results for all 19 samples are also reported through NOAA DIVER as surrogate corrected results. Several samples had TPH concentrations below the sample-specific reporting limit (i.e., concentrations were J-qualified and considered estimates); these were converted to non-detected in DIVER, but were utilized as reported herein.

In addition, separate aliquots of each of the trap samples were analyzed for particulate organic and inorganic matter (POM, PIM), as well as for biogenic silica (BSi) and lithogenic minerals. Replicate sample splits were filtered onto pre-weight and pre-combusted (450ºC for 4-6 hours) 25 mm GF/F filters, briefly rinsed with Milli-Q water and dried at 60ºC before reweighing (total dry weight). Subsequently the filters were combusted at 450ºC for 4-6 hours to remove organic matter and reweighed again yielding mass of PIM. POM was calculated as the difference between the total dry weight and PIM. Replicate filters (25 mm GF/F) were used to determine particulate inorganic carbon (PIC) as the difference of the acidified (fumed with 10% HCl) and non-acidified particulate carbon, analyzed using a CHN elemental analyzer (model CEC 44OHA by Control Equipment; now Exeter Analytical) following Shipe and Brzezinski (2003). Subsamples of the splits were also filtered onto 0.6 µm polycarbonate filters for BSi analysis (Mortlock and Froelich, 1989). Briefly, filters were hydrolyzed with Na_2CO_3 running a 0.5 to 5 hour time series and analyzed colorimetrically. The time series allows corrections for beginning lithogenic silica dissolution during hydrolysis of BSi. The concentration of lithogenic material was calculated by subtracting PIC and BSi from PIM.

Oil Deposition Flux

Hydrocarbon sedimentation rates (flux) for TPH, TPAH16, TPAH50, and hopane ($\mu g/m^2/day$) were calculated by multiplying the concentration of these hydrocarbons in trap samples ($\mu g/g_{dry}$) by the total mass of particles in the trap samples (g_{dry}) divided by 0.5 m^2 (surface area of the trap) then divided by the days deployed (days):

$$\text{Flux } (\mu g/m^2/day) = [(\text{Conc } \mu g/g_{dry}) \times (\text{Mass } g_{dry})] \div 0.5\ (m^2) \div \text{days} \qquad \textit{Eq. (1)}$$

Hopane (17α(H),21β(H)-hopane) was one of the targeted petroleum biomarkers, which is recognized to be highly recalcitrant to oil weathering processes (Prince et al., 1994). The sedimentation rate of hopane in the trap samples was used to estimate the sedimentation rates of Macondo oil on a mass ($kg/km^2/day$) and volume ($barrels/km^2/day$) basis using the previously-determined concentration of hopane (68.8 µg/g; Stout, 2015a) and density (0.856 g/ml at 5°C; Stout, 2015b) of fresh Macondo oil.

Sedimentation rates of POM, PIM, BSi and lithogenic material were calculated from measured concentrations and filtered volume taking split size, the surface area of the trap and the deployment interval into account.

Depletion of Steranes

The loss (depletion) of selected dia- and regular steranes in the sediment trap samples was determined based upon mass losses relative to hopane, which (as noted previously) has proven recalcitrant to biodegradation (Prince et al. 1994). The percent depletions of these selected biomarkers in the trap samples were calculated using the following formula:

$$\%\text{Depletion of S} = [((S_0/H_0) - (S_s/H_s))/(S_0/H_0)] \times 100 \qquad \textit{Eq. (2)}$$

Where S_s and H_s are the concentrations of the selected steranes and hopane in the trap sample, respectively, and S_0 and H_0 are the concentrations of the selected steranes and hopane in the average, fresh Macondo source oil (Stout, 2015a). Although hopane can be degraded under some circumstances, if it (H_s) were in a given sample any % depletions calculated are underestimated.

As is common practice, and in order to eliminate the effects of varying surrogate recoveries on the percent depletion calculations, non-surrogate corrected concentrations are used in these calculations.

Results and Discussion

The results are presented in four sections. The first section briefly introduces the temporal sequence of hydrocarbon concentrations in the sediment trap samples. The second section details chemical characteristics of these hydrocarbons, i.e., their chemical fingerprints. Together these results show that increasingly weathered Macondo oil arrived at the trap in varying but overall decreasing concentrations during the study. In the third section, the sedimentation rate (flux) of hydrocarbons (and, thus oil) are presented and discussed in the context of sedimentation rates of organic and inorganic particles (POM, and biogenic silica and lithogenic minerals), as a means to better understand the specific mechanisms by which oil was transported to the seafloor during the study period. Finally, the fourth section considers the calculated flux of Macondo oil in the trap samples relative to that which is evident in seafloor sediments below the trap as a means to assess the mass/volume of oil deposited before and after the trap was in place.

1: Hydrocarbon Concentrations

Figure 2 shows the temporal trends in the concentrations of TPH, TPAH50, and hopane in the trap samples over the study period. Tabulated data are given in Table 3. Each trend shows an overall decrease in hydrocarbon concentration of trap material over the sampling time, which spanned from six weeks to 14 months after the Macondo well was sealed. During the overall decline in hydrocarbons concentrations, three clear maxima are observed in the Cups 1, 6, and 11 sampling periods (Fig. 2). Although these maxima do not alone indicate "pulses" of oil arriving at the trap, the corresponding TPH, TPAH50, and hopane sedimentation rate data (discussed later in this report) confirm these concentration maxima correspond to periods of higher oil deposition and therefore, are referred to as "pulses" in Figure 2 and hereafter. In addition, the minor maximum observed in Cup 15 is also considered as a fourth, albeit minor, "pulse" of oil (Fig. 2).

The specific chemical character of the hydrocarbons arriving at the trap is discussed in the next section.

2: Hydrocarbon Characteristics

Total Petroleum Hydrocarbons

The chemical fingerprints of the TPH found in the trap samples is revealed by their GC/FID chromatograms. Examples of these, specifically representing the times of the four "pulses" described above (Fig. 2), are shown in Figure 3.

The TPH in Cup 1 (Pulse 1) was dominated by a broad unresolved complex mixture (UCM) spanning from around C_{15} to C_{40}, reaching a maximum around C_{34} (Fig. 3A). The UCM is a long-recognized feature of weathered petroleum (e.g., Gough and Rowland, 1990), indicating the clear presence of weathered crude oil in the Cup 1 sample. Resolved compounds atop the UCM include oil-derived acyclic isoprenoids (pristane and phytane). Shorter-chain n-alkanes are largely absent although longer-chain (n-C_{28}+) n-alkanes are still present. The presence of these long-chain n-alkanes in weathered crude oil is attributed to their lower susceptibility to biodegradation, particularly in marine oil spills (Heath et al., 1997; Peters et al., 2005), which tends to preserve the "high" solid n-alkanes due to steric hindrance effects (Setti et al., 1993). Also present are numerous (mostly) later-eluting resolved compounds, which full scan GC/MS analysis revealed include squalene and multiple (unidentified) unsaturated, highly-branched isoprenoids and cyclic terpenoids (triangles, Fig. 3A). These compounds are biogenic and associated with recent marine biomass (not oil), which was particularly abundant in the Cup 1 sample (see photo; Fig. 2) due to a sinking diatom bloom that occurred in late August 2010 (see later discussion of POM and biogenic silica sedimentation rates).[3]

The TPH in Cup 6 (Pulse 2; Dec. 2010) and Cup 11 (Pulse 3; April 2011) also exhibited broad UCMs consistent with weathered crude oil, although their UCMs are somewhat higher boiling than that of Cup 1 (Fig. 3B-C). This is consistent with the Cup 6 and Cup 11 oils being more highly weathered (biodegraded) than the oil in Cup 1, a feature also indicated by the absence of pristane or phytane. In addition to containing a suite of biogenic isoprenoids and terpenoids, the oil in Cups 6 and 11 also contained prominent long-chain n-alkanes ranging from about n-C_{28} to n-C_{45}, reaching a maximum around n-C_{33} range (Fig. 3B-C). These long-chain n-alkanes exhibit no odd-over-even predominance typical of modern plant waxes, but instead appear typical of oil. As in the Cup 1 oil, the presence of these long-chain n-alkanes in weathered crude oil is attributed to their preservation during biodegradation (Setti et al., 1993; Heath et al., 1997). In total, the shift in the UCM toward higher masses, the absence of pristane and phytane and the greater prominence of long-chain n-alkanes in the Cup 6 and 11 are all consistent with an increased level of biodegradation of the crude oil arriving at the trap during Pulses 2 and 3, as compared to Pulse 1 (Cup 1). The fact that the oil arriving at the trap over time was increasingly biodegraded is consistent with the advancement in weathering of Macondo oil present within the water column – rather than the arrival of some other oil at a single level of weathering such as might be episodically released from natural oil seeps.

The weathered character of the oils found in the trap samples are consistent with those exhibited by the Macondo oil found widespread on the seafloor following the Deepwater

[3] Microscopic examination revealed this biomass was largely comprised of the diatom, *Skeletonema*.

Horizon oil spill (Stout, 2015e). For example, Figure 3F shows the GC/FID chromatogram for a surface sediment (0-1 cm) collected in May 2011 and located about 1 km southeast of the sediment trap studied. This sample is typical of the seafloor floc containing Macondo oil that was found in surface sediments throughout the deep-sea following the *Deepwater Horizon* oil spill (Stout, 2015e). As can be seen, the seafloor floc (Fig. 3F) exhibits the same general features as the oil found in the Cup 6 and Cup 11 sediment trap samples (Fig. 3B-C), *viz.*, broad UCM, no pristane or phytane, and prominent long-chain n-alkanes. These characteristics (and the PAH and biomarker discussed below) indicate the oil present in the sediment trap samples collected between August 2010 (Fig. 3A) and (at least) April 2011 (Fig. 3C) is weathered Macondo oil comparable to that found in seafloor floc deposited throughout the deep-sea (Fig. 3F).

After April 2011, the trap samples collected contained increasingly lower concentrations of TPH (Fig. 2). As such, the GC/FID chromatograms of these later samples contained less-and-less of an UCM and long-chain n-alkanes, and more-and-more biogenic material considered typical of marine biomass. For example, only traces of an oil-derived UCM and long-chain n-alkanes are still present the Cup 15 sample (Pulse 4/June 2011), which is instead dominated by biogenic material (see triangles, Fig. 3D). Thus, although present in lower concentrations (Table 3; Fig. 2), the trap samples collected after April 2011 (Cups 13 to 18) still appeared to contain traces of highly weathered oil (e.g., Fig. 3D). Only the last sample analyzed (Cup 19) contained no recognizable traces of a petroleum-associated UCM or long-chain n-alkanes (Fig. 3E). Cup 19's TPH appears entirely attributable to biogenic material.

Polycyclic Aromatic Hydrocarbons (PAHs)
As the concentration of total PAHs (TPAH50) declined over time (Fig. 2), the distribution of individual PAHs in the trap samples also varied over time. Fig. 4A-E shows the PAH concentration histograms for the same five trap samples that were shown in Figure 3A-E. The first four of these represent the multiple "pulses" of oil arriving at the trap (as described above), and like the TPH, these oils exhibit increasing levels of weathering over time.

The progression in PAH weathering evident in the Cup 1 through Cup 15 (Fig. 4A-D) was evident in the increasing abundances of higher molecular weight PAHs and PAHs with higher degrees of alkylation. Eventually the high molecular weight benz(a)anthrancenes and chrysenes (BC1-BC3) became the most abundant of the PAHs present (Fig. 4D). This progression is typical of weathering of crude oil due to the combined effects of dissolution and biodegradation, both of which tend to preserve higher molecular weight PAHs with higher degrees of alkylation (Elmendorf et al., 1994). Thus, the PAHs in the oil arriving at the trap over time were increasingly weathered, which as noted for TPH, is consistent with a progression in the weathering of Macondo oil within the water column. This observed pattern is not consistent with the appearance of another oil episodically released from seeps.

Notably, the Cup 1 (Pulse 1) oil contained a prominence of alkylated decalins (D0-D4) that exceeded the concentration of naphthalenes (N0-N4; Fig. 4A). This is notable because the concentration of naphthalenes far exceeds that of decalins in the fresh Macondo oil (Stout, 2015a). Naphthalenes are more soluble than, but comparably volatile with decalins. It is obvious that naphthalenes have been dramatically reduced in the Cup 1 oil compared to decalins (Fig. 4A), which indicates that the oil in this sample has been water-washed but not significantly evaporated. Because oil that had reached

the surface (and subsequently sunk) would have likely experienced greater loss of decalins due to evaporation, the decalins' relative prominence in the Cup 1 sample's oil indicates that most of the Macondo oil present could not have come from the sea surface, as otherwise decalins would have appeared more evaporated. We interpret this to mean that the oil found in Cup 1 was more likely derived from water-washed oil from the deep-sea plume (and not from evaporated and water-washed oil that had sunk from the sea surface). This perhaps makes sense since floating surface oil had dissipated by late August 2010 (when Cup 1 was collected). The same might be concluded for the Cups 6 and 11 oils, which also retained traces of decalins, though in declining abundances (Fig. 4B-C). The later arriving oil in Cup 15 was too highly weathered to make this type of distinction (but clearly no floating surface oil was still present in the region by June 2011).

The last trap sample studied (Cup 19; Sept. 2011) contained the lowest measured concentration of TPAH50 (0.064 μg/g), most of which was comprised of Priority Pollutant (i.e. non-alkyl substituted) TPAH16 (0.048 μg/g; Table 3; Fig. 4E). As evident in the TPH results (Fig. 3E), the PAH results also provide no evidence for any oil present in this sample. Instead, the Priority Pollutant PAHs present in this sample at low levels, and virtual absence of alkylated PAHs, are more reasonably attributed to a "background" deposition of riverine or atmospheric combustion particles, which are known to be enriched in Priority Pollutant PAHs (Blumer and Youngblood 1975), and are presumably falling out and sinking in the deep-sea at a low background rate.

Not surprisingly the general character of the PAHs in the trapped oils closely matched the character of PAHs in the Macondo oil (oily floc) found in surface sediments throughout the deep sea (Stout, 2015e). For example, Figure 4F shows the average PAH distribution for seafloor oily floc (0-1 cm) collected from 20 cores located three to five miles from the Macondo wellhead (Stout, 2015e), i.e., about the same distance as the sediment trap studied herein. Like the trap samples containing oil (Fig. 4A-D), PAHs in the oily floc from the seafloor also are dominated by C_3- and C_4- alkylated benz(a)anthracenes and chrysenes, with increasingly lower abundances of alkylated fluoranthrenes/pyrenes, phenanthrenes/anthracenes, naphthalenes, and alkylated decalins (Fig. 4F). Thus, as was the case with the TPH, the PAHs found in the trap samples collected between late August 2010 and April 2011 (Pulses 1 to 3; Fig. 4A-C), and potentially even longer (Pulse 4; Fig. 4D), are consistent with increasingly weathered Macondo oil (Fig. 4F).

Unique among the samples studied, Cup 1 contained prominent Priority Pollutant (non-alkylated parent) PAHs, as indicated by the arrows shown in Fig. 4A and the higher TPAH16 concentrations (Table 3). These apparently "extra" non-alkylated PAHs are not reasonably attributable to petrogenic sources and markedly exceed the concentration of Priority Pollutant PAHs present in the Cup 19 "background" sample. It is well established that Priority Pollutant PAHs, particularly high molecular weight non-alkylated PAHs, are abundant in partially combusted organic matter, including partially combusted oil (e.g. Blumer and Youngblood 1975; Wang et al 1999). Therefore, we attribute "extra" Priority Pollutant PAHs in the Cup 1 trap sample (only; Fig. 4A) to the sedimentation of combustion particles derived from the *in situ* burning (ISB) of floating Macondo oil, which was used as a countermeasure in response to the *Deepwater Horizon* oil spill. Specifically, between April 28 and July 19, 2010 approximately 220,500 to 310,400 barrels (bbls) of floating Macondo crude oil reportedly were consumed in 411 separate ISB events (Mabile and Allen, 2010; Perring et al., 2011). At least some

fraction of the uncombusted emissions from these fires returned to the sea surface and settled through the water column. The "extra" Priority Pollutants present in the late August-early September trap material (Cup 1; Fig. 4A; Table 3) thereby likely reflects the sinking of combustion particles from the ISB events, as is also confirmed by measurements of black carbon (Yan et al. 2015). The fact that the last ISB events occurred in mid-July 2010, and that "extra" Priority Pollutant PAHs were not observed after late August-early September (Cup 1), indicates that combustion particles from the ISB events apparently did not "linger" in the atmosphere or water column for more than 5 or 6 weeks.

Finally, it is notable that the absolute concentration of perylene in the trap samples was generally constant throughout the sampling period except for those samples collected in Cups 1 and 10, which contained about twice as much perylene as the other samples (Table 3). Perylene is considered a biogenic PAH, derived from multiple sources of biomass, including diatoms (Venkatesan, 1988). Cups 1 and 10 each also demonstrated elevated fluxes of biogenic silica (see below), which is consistent with elevated diatom biomass. Sinking diatom blooms are frequently responsible for maximal sedimentation rates, and it is therefore perhaps not surprising that Cups 1 and 10 each, which had the highest concentrations of perylene and BSi, also contained the highest total masses of particulate material measured as dry weight (Table 1). Interestingly, the diatom bloom events represented in Cups 1 and 10 also coincide with Pulses 1 and 3 (Fig. 2; Table 3), which suggests sinking diatom biomass from these blooms appear efficient at "scavenging" the lingering Macondo oil and combustion products from the water column. This mechanism for transporting oil to the seafloor is further discussed later in this report.

Petroleum Biomarkers

As noted above, hopane concentrations in the trap samples decreased over the sampling period with minor increases generally coincident with "pulses" in TPH and PAH (Fig. 2; Table 3). Hopane, of course, is only one of the targeted biomarkers present in crude oil – and in the case of the trap samples studied, hopane was the most abundant biomarker detected. Its dominance can be seen in Figure 5, which shows hopane-normalized histograms of all targeted biomarkers in the same five trap samples shown in Figures 3 and 4. For comparison, also shown in Figure 5 are the average biomarker distributions for fresh Macondo oil (Stout, 2015a) and for Macondo oil collected from the seafloor surface (0-1 cm) of 20 cores three to five miles from the Macondo well (Stout, 2015e).

Inspection reveals that there is an overall similarity between the biomarkers in the trap samples and those of fresh Macondo oil and/or Macondo oil (oily floc) on the seafloor. However, there are some differences between the oil in the trap samples versus the fresh Macondo oil or oily seafloor floc for each of the three classes of biomarkers, *viz.*, triterpanes (blue), diasteranes and steranes (red), and triaromatic steroids (TAS; yellow). Without further consideration these biomarker differences might be blindly interpreted to indicate that different (non-Macondo) oil is present in the trap samples. However, this is not the case. The observed differences are attributable to (1) interferences with biomarkers derived from recent marine biomass in the trap samples or (2) the effects of weathering, *viz.*, biodegradation and dissolution, as discussed in the following paragraphs.

With respect to the triterpanes, various terpenoids were clearly evident in the GC/FID chromatograms of the trap samples (Fig. 3). Recent sediments contain terpenoids derived from modern algal and/or microbial biomass, including numerous hopenes and 17β(H),21β(H)-hopanes (Simoneit 1986; Hood et al. 2002). These modern terpenoids can interfere and co-elute with targeted (oil-derived) biomarkers within *m/z* 191 mass chromatograms (not shown). Under the GC/MS conditions used for this study modern terpenoids co-elute with at least four targeted biomarkers (T11a, T20, T26, and T35; Table 2), which are indicated by the light-blue stippled bars in Figure 5. The largest of these occurs at T20 (moretane; Fig. 5) and is likely due to the co-elution of 17β(H),21β(H)-30-norhopane, a naturally-occurring triterpane, which can be prominent in recent marine sediments (Kennicutt and Comet, 1992). Thus, the prominence of these modern terpenoids (mostly biohopanoids) in the trap samples is attributed to modern biomass and not the presence of a "different" type of crude oil.

Minor differences in sterane distributions are also likely affected by the presence of modern marine biomass in the trap material. However, significant differences between the trap samples and fresh Macondo oil and seafloor floc containing Macondo oil appear in the relative abundances of C_{27} βα-diasteranes (S4 and S5) and C_{27} ββ-steranes (S14 and S15; Table 2; Fig. 5).[4] Specifically, the abundances of these compounds in the trap samples appear intermediate between the fresh Macondo oil and seafloor floc. In addition, the relative abundances of these diasteranes and steranes tend to decrease in the trap samples over time. This temporal trend can be seen in the few examples of trap oils shown in Figure 5A through 5D, but is more easily seen in Figure 6, which shows the calculated percent depletions of C_{27} βα-diasteranes (S4 and S5) and C_{27} ββ-steranes (S14 and S15) for all 19 of the trap samples studied. The progressive loss of these compounds is clearly evident in Cups 1 through 8 (late August 2010 to late January 2011) and appears to continue, albeit with some scatter, thereafter (Fig. 6).

As is evident in Figure 5 (see black dashed lines), the C_{27} βα-diasteranes and C_{27} ββ-steranes were significantly depleted within the widespread seafloor floc found in surface sediments (Stout, 2015e). A comparable loss of βα-diasteranes and ββ-steranes was also reported by White et al. (2012) for the Macondo oil within floc found on deep-sea coral samples collected from northeast Biloxi Dome in later 2010. The preferential loss of C_{27} βα-diasteranes and/or C_{27} ββ-steranes has been previously observed in highly biodegraded oils from the environment (Wang et al., 2001; Prince et al. 2002) and *in vitro* (Diez et al., 2005). Thus, these compounds' progressive depletion in sinking oil (Figs. 5 and 6) and their depletion in floc from the seafloor or deep-sea coral, is attributed to biodegradation of the Macondo oil (and not the presence of a "different" type of crude oil). This progressive loss of C_{27} diasteranes and ββ-steranes is consistent with the progressively weathered character of the TPH and PAH present in the trap samples (Figs. 3 and 4; see above).

As per the TPH and PAH, the gradual depletion of dia- and regular C_{27} steranes in the oil arriving at the trap (Fig. 6) is important as it shows the oil arriving at the trap was progressively weathered over the study period – despite at least some of the oil arriving in "pulses". Increasingly weathered oil arriving at the trap over time would be consistent with oil released from the *Deepwater Horizon* oil spill, which progressively weathered

[4] Some loss of the C_{27} αα-steranes are also suspected (S12 and S17; Fig. 5). However, because these compounds co-elute with C_{29} diasteranes (S13 and S18) the observed depletion cannot confidently be attributed to the loss to any one compound.

during its residence time in the water column. On the other hand, the arrival of increasingly weathered oil would be inconsistent with an oil that was released episodically from a natural oil seep. Thus, the progression in sterane weathering over time (Fig. 6) is a convincing line of evidence that the arriving oil was from the *Deepwater Horizon* oil spill, and not from a natural oil seep.

Finally, the most obvious difference between the biomarkers in the oil from trap material and fresh Macondo oil or Macondo oil found in seafloor floc is the significant depletion of all four TAS congeners measured in the trap material (see yellow bars; Fig. 5). The cause for this difference is interesting given the otherwise high similarity between the oil from trap samples and Macondo oil in seafloor floc (e.g., Figs. 3 and 4). Given the other changes due to weathering on TPH, PAH and other biomarkers described above, some form of weathering must be responsible for the depleted TAS, as discussed in the following paragraphs.

Given their condensed aromatic structures, TAS are considered susceptible to photo-oxidation and were observed to be variably depleted in floating and stranded Macondo oils (Aeppli et al., 2014; Stout, 2015c,d). However, photo-oxidation also affects other *uv*-sensitive compounds; e.g., an enrichment of chrysene and methyl-chrysenes relative to C2+ chrysenes has been observed in photo-oxidized oils (Garrett et al., 1998). No such enrichment is evident in the trap samples (Fig. 4) arguing that photo-oxidation could not explain the depleted TAS in the trap samples. Furthermore, photo-oxidation would mandate that the oil within the traps had once been at the sea surface, which does not seem likely given the general lack of evaporation of the decalins (at least in the Cup 1 sample; Fig. 4A, see discussion above). Evaporation of the TAS can also be ruled out given the lack of evaporation among many more volatile constituents in the trap samples.

This leaves biodegradation or dissolution as possible causes for the depletion of TAS found in the oil within the trap samples. We believe that both processes could have affected the Macondo oil arriving at the trap. As explained in the next section, we contend that the oil collected in the trap represents the "lingering" fraction of oil that remained within the water column long after the spill. (Most oil that had been present within the water column during the active spill was previously scavenged by marine snow or otherwise deposited on the seafloor, or transported out of the area study.) Theoretically, this "lingering" oil may have experienced greater degrees of dissolution or biodegradation due to its longer residence in the water column. Both dissolution and biodegradation of TAS in the "lingering" oil may also have been enhanced if the "lingering" oil consisted of smaller droplet sizes. Specifically, smaller oil droplet size would have larger surface area-to-volume ratios, allowing greater dissolution and/or biodegradation to occur at their surfaces. Smaller droplet size might also have allowed for longer residence within the water column, because smaller particles are less likely to encounter sinking marine snow, whereas larger oil droplets would be scavenged and deposited on the seafloor more quickly. Therefore, at present, we contend the most likely explanation for the greater depletion of TAS in the oils within the trap samples (versus TAS in seafloor floc) lies in the apparent longer residence time of oil within the water column, and perhaps smaller droplet size.

3: Sedimentation Rates (Fluxes) of Oil and Marine Particles

The presence of Macondo oil in the trap samples provides an opportunity to assess the sedimentation rate of oil to the deep-sea floor between about 6 weeks and 14 months

after the Macondo well was sealed (July 20, 2010) ending the spill. In addition, the relative sedimentation rates of oil versus "non-oil" particulates provides a means to assess the mechanism(s) by which oil was carried to the seafloor during this period.

Several lines of evidence indicate that the Macondo oil collected in trap samples stemmed from the water, rather than being resuspended into the trap from the seafloor below. (1) Microscopical investigations revealed that a significant fraction of the diatoms causing the large sedimentation event in September 2010 (cup 1), were intact cells, not just empty or broken frustules. The clear dominance of one species also is typically for a sinking bloom, not for resuspended material (Yan et al. 2015). (2) Whereas planktonic foraminifera were found abundantly in all cups, benthic species were absent except in cups 13, 14, and 18, where they contributed less than 1% of all foraminifera (Yan et al. 2015). (3) Resuspension to more than 100 m above the seafloor requires high current speeds, but the northern Gulf of Mexico was free from large storm events during this time. (4) The overall decreasing trend of oil (Fig. 2) sedimentation could not be explained if resuspension caused the input of this material into traps, as these substances were still layered on the seafloor long after our trap was retrieved. (5) The fingerprint of the oil collected in the trap showed a different weathering process than the oil collected from the seafloor (e.g., TAS).

Table 4 contains the sedimentation rates calculated for TPH, TPAH50, and hopane for the trap samples studied. These rates are plotted in Figure 7, and akin to the concentration trends discussed earlier (Fig. 2), two patterns are evident in these sedimentation rates. First, there is an overall decline in the amount of oil reaching the trap over the entire study period, late August 2010 to September 2011 (6 weeks to 14 months after the end of the spill). Second, superimposed on the overall decline there were "pulses" of higher oil sedimentation rates that clearly occurred on three occasions (Pulses 1 to 3) and less clearly on a fourth occasion (Pulse 4; Fig. 7).

Chemical fingerprinting demonstrated that the oil reaching the trap was consistent with increasingly weathered Macondo oil, derived (at least mostly if not exclusively) from oil within the deep-sea plume. Based upon the combined evidence of the overall declining sedimentation rates following the spill, and the character and progression in weathering of the oil that reached the trap over time, it is evident that "lingering" Macondo oil was still present in the water column (and being transported to the seafloor) in decreasing amounts over the time period spanning from Cup 1 (late August 2010) to Cup 18 (late August 2011). This means that Macondo oil was still being transported to the seafloor for up to 13 months after the spill had ended. Only in Cup 19 (early Sept. 2011) was there no clear evidence for the presence of Macondo oil.

The overall decline in oil sedimentation rates over the time (Fig. 7) is likely attributed to increasingly less oil remaining in the water column above the trap. That is, after the spill any oil in the water column would naturally disperse over time. Natural dispersion would predictably result in a uniform decline in oil reaching the trap. However, because distinct "pulses" of oil deposition (e.g., Cups 1, 6, 10-12, and 15; Fig. 7) also occurred, factors other than how much oil was present in the water column at any given time must have also played a role in determining the sedimentation rates of oil to the seafloor.

It is possible that the observed pulses of higher oil sedimentation could have been caused by varying amounts of oil within the water column (above the trap) due to some oscillation of the vestiges of the advecting deep-sea plume (e.g., passing by the trap during pulses). We have no evidence that such oscillation occurred during the Cups 1, 6, 10-12, or 15 sampling periods. However, we do find relationships exist between the

distinct “pulses” of oil deposition and the *amount* and *type* of “non-oil” particles found within the trap samples. These relationships are not unexpected since sinking marine particles, e.g. marine snow, can efficiently collect suspended particles and dissolved substances within the water column (Passow 2014, Passow et al. 2014, De La Rocha et al. 2008; Smetacek, 1985), including potentially “scavenging” any “lingering” oil (both particulate and dissolved).

Evidence for the role of “non-oil” particles can be seen in the positive correlation between the sedimentation rate of hopane (a proxy for oil deposition independent of weathering due to its conservative nature) and the rates for particulate matter (PIM and POM) reaching the trap (Fig. 8A; data from Table 4). This correlation indicates that during the study period more “lingering” oil was being carried to the seafloor during periods when higher amounts of particles were sinking. This correlation is very clear for the three major “pulses” of oil sedimentation (Pulses 1 to 3; Cups 1, 10, 10-12), whereas the last minor pulse (Pulse 4; Cup 15) appears to lag slightly behind a period of higher particle sedimentation. Notably, however, it is observed that over time the sedimentation rate for oil (hopane) decreases relative to those for PIM or POM, indicating less-and-less “lingering” oil remained in the water column over time. This would seem to make sense as sinking particles (and perhaps other processes) progressively removed more-and-more of the oil from the water column.

The efficiency at which different *types* of sinking particles scavenged “lingering” oil appears to also have played a role. Figure 8 shows the relationships between the sedimentation rate of oil (hopane) and the rates for POM, lithogenic minerals and biogenic silica (data from Table 4). Sedimentation rates of POM and PIM peaked at each “pulse” of hopane sedimentation. Minerals (PIM) and oil may directly form sinking particles, called oil-mineral aggregates (Omotoso et al. 2002, Stoffyn-Egli and Lee 2002), if they co-occur. However, the associated peak POM fluxes at each hopane sedimentation “pulse”, suggest that the formation of oil-mineral aggregates may not have been a dominating the flux events observed here. Instead we propose that sinking marine snow largely drove sedimentation pulses of oil (hopane) and minerals (Passow 2004): Sinking marine snow potentially accumulates oil and non-sinking minerals dispersed over a large depth range, whereas the formation of oil-mineral aggregates requires relatively high concentrations of oil and minerals to co-occur at one depth. In fact a close correlation between sedimentation of POM and lithogenic minerals ($r = 0.91$; $n = 19$; $p < 0.001$) suggests that the presence or absence of marine snow formed from organic marine particles drove all observed sedimentation “pulses” during the investigated time period. It is notable that the sedimentation of oil during Pulses 1 and 3 was also accompanied by increased sedimentation of biogenic silica (Fig. 8B), whereas increased sedimentation of biogenic silica was lacking during Pulse 2 (Cup 6) and 4 (Cup 15). We interpret this difference to indicate that diatom blooms (biogenic silica) played an important role in scavenging the “lingering” oil during Pulses 1 and 3. Diatom aggregates scavenge suspended minerals they encounter during sinking, resulting in the co-sedimentation of lithogenic minerals and biogenic silica in the presence of deep nephloid layers (Kumar et al. 1998, Passow et al. 2001) or atmospheric or riverine input of suspended minerals (Ternon et al. 2010). Diatom aggregates may also efficiently incorporate oil (Passow 2014) and carry it to depth (Parsons et al., 2014). In contrast, sedimentation during Pulse 2 (December 2010) and Pulse 4 must have been driven by non-diatom sinking marine snow consisting for example of zooplankton feeding structures, *Trichodesmium* sp. or miscellaneous organic detritus (Alldredge and Silver 1988).

Finally, the sedimentation rate of TPAH16 (i.e., Priority Pollutant PAHs) in the trap samples is largely unrelated to the sinking of Macondo oil, but is included in Table 4 because it clearly demonstrates the high rate of deposition of combustion particles in late August/early September 2010 (Cup 1) attributed to the *in situ* burning events (Fig. 4A; described above). Specifically, the TPAH16 sedimentation rate during late August/early September (Cup 1) was 0.62 μg/m^2/d, which is more than 10-times higher than the average of all subsequent sampling intervals (0.05 ± 0.03 μg/m^2/day) and 20-times higher than existed one year later (0.03 μg/m^2/day; Table 4). As described above, we attribute the "extra" Priority Pollutant PAHs in Cup 1 to the sinking of combustion particles generated from *in situ* burning of surface oil during the response to the spill. Because the last *in situ* burning occurred July 19 (~5-6 weeks prior to late August/early September), the TPAH16 sedimentation rate(s) prior to late August, and certainly during the active ISB events, were likely even higher.

4: Mass and Volume of Macondo Oil Deposited based on Trap Results

The observed hydrocarbon sedimentation rates (Table 4) can be converted into the mass or volume of Macondo oil being deposited during the study period. This is best achieved using the sedimentation rate for hopane, a proxy for oil deposition independent of weathering of the oil due to its conservative nature. Specifically, because the concentration of hopane in the fresh Macondo oil is known (68.8 mg/kg; Stout, 2015a), the mass of Macondo oil represented in the trap samples can be calculated from the hopane sedimentation rates for each sampling interval. In addition, because the density of fresh Macondo oil is also known (0.8560 g/cm^3 at 5°C; Stout, 2015b), the volume can be similarly calculated.

The results of these calculations – for both mass and volume – are shown in Table 5 for each of the 21-day sampling intervals. Cup 19 is not included since the chemical results provide no basis to indicate Macondo oil was present in this "last analyzed" trap sample. The cumulative totals for Cups 1 to 12, i.e., the time period spanning the three major "pulses" of oil deposition, indicates that approximately 430 kg or 3.2 barrels (bbl) of Macondo oil were deposited in the km^2 beneath the trap between late August 2010 through April 2011. These amounts represent about 86% of the total oil deposited over the trap's entire sampling period (499 kg and 3.7 bbl; Table 5). About 20% of the total oil deposited occurred within Pulse 1.

A cumulative total of 3.2 to 3.7 bbl of oil per km^2 may not seem particularly significant. However, it must be remembered that the sediment trap only began collecting samples six weeks *after* the Macondo well was shut-in (July 15, 2010) and the leak had stopped. Therefore, we contend the trap samples only represented the vestiges of the "main" marine oil snow sedimentation and flocculent accumulation (MOSSFA) event that accompanied the *Deepwater Horizon* oil spill. That is, the sediment trap sampled the late season "dustings" of marine oil snow and missed the "blizzard of the century".

To assess this further, the concentration of Macondo-derived (non-background) hopane of the seafloor surface (0-1 cm) in cores taken in the same area as the trap was deployed – as calculated in another study (Stout et al., 2015) – were determined. For the 4 km^2 area around the sediment trap the average (excess, non-background; ± σ) Macondo-derived hopane concentration in the 0-1 cm interval was determined to be 93 ± 62 μg/kg of sediment (Fig. 9). As per Stout et al. (2015; which assumes a bulk density of the oily floc of 0.105 g/cm^3), this concentration of hopane on the seafloor's surface indicates that the total volume of Macondo oil deposited in the km^2 beneath the trap was on the order of 104 ± 69 bbl.

The large disparity between the volume of Macondo oil on the seafloor (104 ± 69 bbl) and the volume of Macondo oil that was deposited after late August (~3.2 to 3.7 bbl) suggests that only a small percentage of oil was deposited on the seafloor ~4 km southwest of the well was deposited *after* late August 2010 (when the trap sampling started), on average, only ~3% (3.2 out of 104 bbl). Oppositely, this indicates that ~97% of the Macondo oil deposited on the seafloor in this area was deposited *before* late August 2010.

Assuming the trap's location largely is representative of the deep sea, the vast majority (~97%) of the Macondo oil deposited on the seafloor during the MOSSFA was deposited before late August 2010, i.e., during the initial marine oil snow "dirty blizzard" and while the subsea plume persisted. The "lingering" oil that remained in the water column after the well was shut-in July 15, 2010 – as represented by the sediment trap results studied herein – then gradually reached the seafloor over the next 13 months (August 2011).

References

Aeppli, Christoph, Robert K. Nelson, Jagoš R. Radović, Catherine A. Carmichael, David L. Valentine, and Christopher M. Reddy, 2014. "Recalcitrance and degradation of petroleum biomarkers upon abiotic and biotic natural weathering of Deepwater Horizon oil." *Environ. Sci. Technol.* **48**: 6726-6734.

Alldredge, A. L. and M. W. Silver, 1988. "Characteristics, dynamics, and significance of marine snow." *Prog. Oceanogr.* **20**: 41-82.

Atlas, Ronald M. and Terry C. Hazen, 2011. "Oil biodegradation and bioremediation: A tale of the two worst spills in U.S. history." *Environ. Sci. Technol.* **45**: 6709-6715.

Blumer, M. and W. W. Youngblood, 1975. "Polycyclic aromatic hydrocarbons in soils and recent sediments." *Science* **188**: 53-55.

Brooks, Gregg R., Rebekka A. Larson, Patrick T. Schwing, Isabel Romero, Christopher Moore, Gert-Jan Reichart, Tom Jilbert, Jeff P. Chanton, David W. Hastings, Will A. Overholt, Kala P. Marks, Joel E. Kostka, Charles W. Holmes, David Hollander, 2015. Sedimentation pulse in the NE Gulf of Mexico following the 2010 DWH blowout. *PLoS ONE* **10(7)**: e0132341. doi:10.1371/journal/pone.0132341.

Camilli, R., C. M. Reddy, D. R. Yoerger, B. A. S. Van Mooy, M. V. Jakuba, J. C. Kinsey, C. P. McIntyre, S. P. Sylva and J. V. Maloney, 2010. "Tracking Hydrocarbon Plume Transport and Biodegradation at Deepwater Horizon." *Science* **330**: 201-204.

Chanton, J., T. Zhao, B. E. Rosenheim, S. B. Joye, S. Bosman, C. Brunner, K. M. Yeager, A. Diercks and D. J. Hollander, 2015. "Using natural abundance of radiocarbon to trace the flux of petrocarbon to the seafloor following the Deepwater Horizon oil spill." *Environ. Sci. Technol.* **49**: 847-854.

De La Rocha, C.L., Nowald, N., Passow, U., 2008. Interactions between diatom aggregates, minerals, particulate organic carbon, and dissolved organic matter: Further implications for the ballast hypothesis. Global Biogeochem Cycles **22**:GB4005.

Diercks, A. R., R. C. Highsmith, V. Asper, D. Joung, Z. Zhou, L. Guo, A. M. Shiller, S. B. Joye, A. P. Teske, N. Guinasso, T. L. Wade and S. E. Lohrenz, 2010. "Characterization of subsurface polycyclic aromatic hydrocarbons at teh Deepwater Horizon site." *Geophys. Res. Letters* **37**(L20602, doi:10.1029/2010GL045046): 6.

Díez, S., Sabate, J., Vinas, M., Bayona, J. M., Solanas, A. M., Albaiges, J., 2005. "The Prestige oil spill. I. Biodegradation of a heavy fuel oil under simulated conditions". *Environ. Toxicol. Chem.* **24**: 2203-2217.

Elmendorf, D. L., C. E. Haith, G. S. Douglas and R. C. Prince, 1994. "Relative rates of biodegradation of substituted polycyclic aromatic hydrocarbons". *Bioremediation of Chlorinated and PAH Compounds*. R. E. L. Hinchee, A.E.\\Semprini, L.\\Ong, S.K. Ann ARbor, Michigan, Lewis Publishers**:** 188-202.

Fisher, C. R., P.-Y. Hsing, C. L. Kaiser, D. R. Yoerger, H. H. Roberts, W. W. Shedd, E. E. Cordes, T. M. Shank, S. P. Berlet, M. G. Saunders, ET AL. Larcom and J. M. Brooks, 2014. Footprint of Deepwater Horizon blowout impact to deepwater coral communities. *Proc. Nat'l. Acad. Sci.* **111**(32): 11744-11749.

Garrett, R. M., I. J. Pickering, C. E. Haith and R. C. Prince, 1998. "Photooxidation of crude oils." *Environmental Science and Technology* **32**(23): 3719-3723.

Gough, M. A. and M. A. Rowland, 1990. "Characterization of unresolved complex mixtures of hydrocarbons in petroleum." *Nature* **344**: 648-650.

Hazen, Terry C., Eric A. Dubinsky, Todd Z. DeSantis, Gary L. Andersen, Yvette M. Piceno, Navjeet Singh, Janet K. Jansson, Alexander Probst, Sharon E. Borglin, Julian L. Fortney, William T. Stringfellow, Markus Bill, Mark E. Conrad, Lauren M. Tom, Krystle L. Chavarria, Thana R. Alusi, Regina Lamendella, Dominique C. Joyner, Chelsea Spier, Jacob Baelum, Manfred Auer, Marcin L. Zemla, Romy Chakraborty, Eric L. Sonnenthal, Patrik D'haeseleer, Hoi-Ying N. Holman, Shariff Osman, Zhenmei Lu, Joy D. Van Nostrand, Ye Deng, Jizhong Zhou, and Olivia U. Mason, 2010. "Deep sea oil plume enriches indigenous oil degrading bacteria." *Science* **330**: 204-208.

Heath, D.J., C.A. Lewis and S.J. Rowland, 1997. "The use of high temperature gas chromatography to study the biodegradation of high molecular weight hydrocarbons". *Org. Geochem*. **26**: 769-785.

Hood, K. C., O. P. Gross, L. M. Wenger and S. C. Harrison, 2002. "Hydrocarbon Systems Analysis of the Northern Gulf of Mexico: Delineation of Hydrocarbon Migration Pathways Using Seeps and Seismic Imaging." *AAPG Studies in Geology* **48**: 25-40.

Hsing, P.-Y., B. Fu, ET AL. Larcom, S. P. Berlet, T. M. Shank, A. F. Govindarajan, A. J. Lukasiewicz, P. M. Dixon and C. R. Fisher, 2013. "Evidence of lasting impact of the Deepwater Horizon oil spill on a deep Gulf of Mexico coral community." *Elementa* **1**(doi: 10.12952/journal.elementa.000012).

Kennicutt, M. C. and P. A. Comet, 1992. "Resolution of sediment hydrocarbons sources: Multiparameter approach". *Organic Matter: Productivity, Accumulation, and Preservation in Recent and Ancient Sediments*. J. K. Whelan and J. W. Farrington. New York, Columbia Univ. Press**:** 309-338.

Kinner, N. E., L. Belden and P. Kinner, 2014. "Unexpected sink for Deepwater Horizon oil may influence future spill response." *EOS* **95**(21): 27.

Kumar, M.D., Sarma, V.V.S.S., Ramaiah, N., Gauns, M., de Sousa, S.N., 1998. "Biogeochemical significance of transparent exopolymer particles in the Indian Ocean". *Geophysical Research Letters* **25**:81-84.

Mabile, N. and Allen, A., 2010. Controlled burns - After-action report. Controlled Burn Group Report, dated Aug. 8, 2010.

Mitra S, Kimmel, D.G., Snyder, J., Scalise, K., McGlaughon, B.D., Roman, M.R., Jahn, G.L., Pierson, J.J., Brandt, S.B., Montoya, J.P., Rosenbauer, R.J., Lorenson, T.D., Wong, F.L., Campbell, P.L., 2012. "Macondo-1 well oil-derived polycyclic aromatic hydrocarbons in mesozooplankton from the northern Gulf of Mexico". *Geophysical Research Letters* **39**: L01605, doi:10.1029/2011GL049505

Montagna, P. A., J. G. Baguley, C. Cooksy, I. Hartwell, L. J. Hyde, J. L. Hyland, R. D. Kalke, L. M. Kracker, M. Reuscher and A. C. E. Rhodes, 2013. "Deep-sea benthic footprint of the Deepwater Horizon blowout." *PLoS ONE* **8**(8): e70540. doi:70510.71371/journal.pone.0070540.

Mortlock, R.A. and P.N. Froelich. 1989. "A simple method for the rapid determination of biogenic opal in pelagic marine sediments". Deep Sea Res. 36(9): 1415-1426

NOAA, 2011. "Joint Analysis Group - Deepwater Horizon oil spill: Review of Preliminary Data to Examine Subsurface Oil in the Vicinity of MC252#1, May 19 to June 19, 2010." *NOAA Technical Report* **NOS OR&R 25**(Silver Spring, MD): 52 p.

NOAA, 2014. Analytical quality assurance plan, Mississippi Canyon 252 (*Deepwater Horizon*) natural resource damage assessment, Version 4.0. May 30, 2014.

North, Elizabeth W., E. Eric Adams, Zachary Schlag, Christopher R. Sherwood, Ruoying He, Kyung Hoon Hyun, and Scott A. Socolofsky, 2011. "Simulating oil droplet dispersal from the Deepwater Horizon spill with a Lagrangian approach". Geophys. Monogr. Ser. 195: 217-226.

Omotoso, O.E., Munoz, V.A., Mikula, R.J., 2002. "Mechanisms of crude oil-mineral interactions". *Spill Sci. Tech. Bull.* **8**:45-54.

Parsons, M.L., Turner, R.E., Overton, E.B., 2014. "Sediment-preserved diatom assemblages can distinguish a petroleum activity signal separately from the nutrient signal of the Mississippi River in coastal Louisiana". *Mar. Poll. Bull.* **85**:164-171

Passow, U., 2004. "Switching perspectives: Do mineral fluxes determine particulate organic carbon fluxes or vice versa". *Geochemistry, Geophysics, Geosystems* 5:1-5

Passow, U., 2014. "Formation of rapidly-sinking, oil-associated marine snow." *Deep-Sea Res*. **Part II, Top. Stud. Oceanogr.**: doi: 10.1016/j.dsr1012.2014.1010.1001.

Passow, U., Shipe, R.F., Murray, A., Pak, D.K., Brzezinski, M.A., Alldredge, A.L., 2001. "Origin of transparent exopolymer particles (TEP) and their role in the sedimentation of particulate matter". *Continental Shelf Research* **21**:327-346.

Passow, U., K. Ziervogel, V. Asper and A. Diercks, 2012. "Marine snow formation in the aftermath of the Deepwater Horizon oil spill in the Gulf of Mexico." *Environ. Res. Lett.* **7**: 11 p.

Passow, U., De La Rocha, C.L., Fairfield, C., Schmidt, K., 2014. "Aggregation as a function of pCO2 and mineral particles". *Limnology and Oceanography* **59**:532-547.

Peters, K.E., Walters, C.C. and J.M. Moldowan, 2005. The Biomarker Guide, Vol. II, Biomarkers and isotopes petroleum systems and Earth history. Cambridge Univ. Press, Cambridge.

Perring, A. E., J.P. Schwarz, J.R. Spackman, R. Bahreini, J.A. deGouw, R.S. Gao, J.S. Holloway, D.A. Lack, J.M. Langridge, J. Peischl, A.M. Middlebrook, T.B. Ryerson, C. Warneke, L.A. Watts, D.W. Fahey, 2011. "Characteristics of black carbon aerosol from a surface oil burn during the Deepwater Horizon oil spill." *Geophys. Res. Letters* **38**(L17809): 5 pp.

Prince, R. C., D. L. Elmendorf, J. R. Lute, C. S. Hsu, C. E. Haith, J. D. Senius, G. J. Dechert, G. S. Douglas and E. L. Butler, 1994. "17a(*H*),21b(*H*)-hopane as a conserved internal marker for estimating the biodegradation of crude oil." *Environmental Science and Technology* **28**(1): 142-145.

Prince, R. C., E. H. Owens and G. A. Sergy, 2002. "Weathering of an Arctic oil spill over 20 years: the BIOS experiment revisited." *Marine Pollution Bulletin* **44**(11): 1236-1242.

Ryerson, Thomas B., Richard Camilli, John D. Kessler, Elizabeth B. Kujawinski, Christopher M. Reddy, David L. Valentine, Elliot Atlas, Donald R. Blake, Joost de Gouw, Simone Meinardi, David D. Parrish, Jeff Peischl, Jeffrey S. Seewald, and Carsten Warneke, 2012. "Chemical data quantify Deepwater Horizon hydrocarbon flow rate and environmental distribution." *Proc. Nat'l. Acad. Sci.* **109**(50): 20246-20253.

Romero, I.C., P.T. Schwing, G.R. Brooks, R.A. Larson, D.W. Hastings, G. Ellis, E.A. Goddard, D.J. Hollander, 2015. "Hydrocarbons in deep-sea sediments following the

2010 Deepwater Horizon blowout in the northeast Gulf of Mexico". *PLoS ONE* 10:e0128371

Shipe, R.F. and M.A. Brzezinski. 2003. "Siliceous plankton dominate primary and new productivity during onset of El Nino conditions in the Santa Barbara Basin, California". Journal of Marine Systems. 42:127-143.

Setti, L., G. Lanzarini, P.G. Pifferi, and G. Spagna, 1993. "Further research into aerobic degradation of n-alkanes in a heavy oil by a pure culture of Pseudomonas spp". *Chemosphere* **26**: 1151-1157.

Simoneit, B. R. T., 1986. "Cyclic terpenoids of the geosphere". *Biological Markers in teh Sedimentary Record*. R. B. Johns. Amsterdam, Elsevier**:** 43-59.

Smetacek, V.S., 1985. "Role of sinking in diatom life-history cycles: Ecological, evolutionary, and geological significance". *Marine Biology* 84:239-251

Sokolofsky, S. A., E. E. Adams and C. R. Sherwood, 2011. "Formation dynamics of subsurface hydrocarbon intrusions following the Deepwater Horizon blowout." *Geophys. Res. Letters* **38**(L09602, doi:10.1029/2011GL047174): 6 p.

Stoffyn-Egli, P. and Lee, K., 2002. "Formation and characterization of oil-mineral aggregates. *Spill Sci.Tech. Bull.* **8**:31-44.

Stout, S.A., 2015a. Detailed chemical characteristics of fresh Macondo crude oil. NewFields technical report to the Trusteees in support of the DARP, August 2015.

Stout, S.A., 2015b. Physical Properties of Fresh and Weathered Macondo Crude Oil. NewFields technical report to the Trusteees in support of the DARP, August 2015.

Stout, S.A., 2015c. Chemical composition of floating Macondo oil during the Spring-Summer of 2010. NewFields technical report to the Trusteees in support of the DARP, August 2015.

Stout, S.A., 2015d. Distribution and weathering of Macondo Oil stranded on shorelines in 2010 based on chemical fingerprinting. NewFields technical report to the Trusteees in support of the DARP, August 2015.

Stout, S.A., 2015e. Chemical evidence for the presence and distribution of Macondo oil in deep-sea sediments following the Deepwater Horizon oil spill. NewFields technical report to the Trusteees in support of the DARP, August 2015.

Stout, S.A. and C. German, 2015. Characterization and flux of marine oil snow in the Viosca Knoll (Lophelia Reef) area due to the Deepwater Horizon oil spill. NewFields Technical Report to DARP, August 2015.

Stout, S.A., S. Rouhani, B. Liu, and J. Oehrig 2015. Spatial extent ("footprint") and volume of Macondo oil found on the deep-sea floor following the *Deepwater Horizon* oil spill. NewFields technical report to the Trusteees in support of the DARP, August 2015.

Ternon, E., Guieu, C., Löye-Pilot, M-D., Leblond, N., Bosc, E., Gasser, B., Miquel, J.C., Martin, J., 2010. "The impact of Saharan dust on the particulate export in the water column of the North Western Mediterranean Sea". *Biogeosciences*, **7(3)**: 809-826.

Valentine, D. L., G. Burch Fisher, S. C. Bagby, R. K. Nelson, C. M. Reddy, S. P. Sylva and M. A. Woo, 2014. "Fallout plume of submerged oil from Deepwater Horizon." *Proc. Nat'l. Acad. Sci.* **10.1073/pnas.1414873111**: 6 p.

Venkatesan, M. I., 1988. "Occurrence and Possible Sources of Perylene in Marine Sediments - A Review." *Marine Chemistry* **25**: 1-27.

Wang, Z., Fingas, M., Shu, Y, Sigouin, L., Landriault, M., and Lambert, P. 1999. Quantitative Characterization of PAHs in Burn Residue and Soot Samples and Differentiation of Pyrogenic PAHs from Petrogenic PAHs - the 1994 Mobile Burn Study. Environmental Science and Technology, 33, pp 3100 - 3109.

Wang, Z., M. Fingas, E. H. Owens, L. Sigouin and C. E. Brown, 2001. "Long-term fate and persistence of the spilled Metula oil in a marine salt marsh environment Degradation of petroleum biomarkers." *Journal of Chromatography A* **926**: 275-290.

White, Helen K., Pen-Yuan Hsing, Walter Cho, Timothy M. Shank, Erik E. Cordes, Andrea M. Quattrini, Robert K. Nelson, Richard Camilli, Amanda W. J. Demopoulos, Christopher R. German, James M. Brooks, Harry H. Roberts, William Shedd, Christopher M. Reddy, and Charles R. Fisher, 2012. "Impact of the Deepwater Horizon oil spill on a deep-water coral community in the Gulf of Mexico." *Proc. Nat'l. Acad. Sci.* **109**(50): 20303-20308.

Yan, B., Passow, U., Chanton, J, Nöthig, E-M., Asper, V., Sweet, J., Pitiranggon, M., Diercks A., Pak, D., subm. July 2015. "Natural marine particles mediated sedimentation of oil and drilling mud components from the *Deepwater Horizon* spill". *Proc. Nat'l. Acad. Sci.*

Table 1: Inventory of sediment trap samples studied. Total mass of particulate material (g dry) collected in each cup is given at the far right.

Sample ID for Plots	Sample ID	Alpha ID	Open Date	Close Date	Mid-Date	Days Deployed	Sample Mass (g wet)	%Solid	Sample Mass (g dry)	Fraction of Total Sample	Total Mass (g dry)
Cup 1	GoM2010-2011_S1_C1_1-16	1304019-01	25-Aug-10	15-Sep-10	4-Sep-10	21	8.41	14.31	1.20	16	19.3
Cup 2	GoM2010-2011_S1_C2_1-8	1308023-01	15-Sep-10	6-Oct-10	25-Sep-10	21	6.37	14.00	0.89	8	7.1
Cup 3	GoM2010-2011_S1_C3_1-8	1308023-02	6-Oct-10	27-Oct-10	16-Oct-10	21	4.00	17.54	0.70	8	5.6
Cup 4	GoM2010-2011_S1_C4_1-8	1308023-03	27-Oct-10	17-Nov-10	6-Nov-10	21	4.47	16.33	0.73	8	5.8
Cup 5	GoM2010-2011_S1_C5_1-8	1308023-04	17-Nov-10	8-Dec-10	27-Nov-10	21	2.36	14.81	0.35	8	2.8
Cup 6	GoM2010-2011_S1_C6_1-8	1308023-05	8-Dec-10	29-Dec-10	18-Dec-10	21	4.74	17.27	0.82	8	6.5
Cup 7	GoM2010-2011_S1_C7_1-8	1308023-06	29-Dec-10	19-Jan-11	8-Jan-11	21	4.34	15.63	0.68	8	5.4
Cup 8	GoM2010-2011_S1_C8_1-8	1308023-07	19-Jan-11	9-Feb-11	29-Jan-11	21	4.04	13.64	0.55	8	4.4
Cup 9	GoM2010-2011_S1_C9_1-8	1308023-08	9-Feb-11	2-Mar-11	19-Feb-11	21	3.71	17.02	0.63	8	5.1
Cup 10	GoM2010-2011_S1_C10_1-8	1304019-02	2-Mar-11	23-Mar-11	12-Mar-11	21	9.14	22.04	2.01	8	16.1
Cup 11	GoM2010-2011_S1_C11_1-8	1304019-03	23-Mar-11	13-Apr-11	2-Apr-11	21	5.13	20.18	1.04	8	8.3
Cup 12	GoM2010-2011_S1_C12_1-8	1308023-09	13-Apr-11	4-May-11	23-Apr-11	21	8.83	11.76	1.04	8	8.3
Cup 13	GoM2010-2011_S1_C13_1-8	1308023-10	4-May-11	25-May-11	14-May-11	21	3.56	14.58	0.52	8	4.2
Cup 14	GoM2010-2011_S1_C14_1-8	1308023-11	25-May-11	15-Jun-11	4-Jun-11	21	5.12	14.00	0.72	8	5.7
Cup 15	GoM2010-2011_S1_C15_1-8	1308023-12	15-Jun-11	6-Jul-11	25-Jun-11	21	4.52	14.14	0.64	8	5.1
Cup 16	GoM2010-2011_S1_C16_1-8	1308023-13	6-Jul-11	27-Jul-11	16-Jul-11	21	4.35	11.86	0.52	8	4.1
Cup 17	GoM2010-2011_S1_C17_1-8	1308023-14	27-Jul-11	17-Aug-11	6-Aug-11	21	4.15	12.24	0.51	8	4.1
Cup 18	GoM2010-2011_S1_C18_1-8	1308023-15	17-Aug-11	7-Sep-11	27-Aug-11	21	3.23	18.52	0.60	8	4.8
Cup 19	GoM2010-2011_S1_C19_1-8	1304019-04	7-Sep-11	28-Sep-11	17-Sep-11	21	4.16	10.58	0.44	16	3.5
J - concentration is estimated; below RL											
NA - not available/not analyzed											

Table 2: Inventory of target analytes for the PAH and petroleum biomarkers quantified in this study. Abbreviations are used in figures throughout the report.

Abbrev	*Analytes*	*Abbrev*	*Analytes*	*Abbrev*	*Analytes*	*Abbrev*	*Analytes*
D0	cis/trans-Decalin	BF	Benzo(b)fluorene	T4	C23 Tricyclic Terpane	S4	13b(H),17a(H)-20S-Diacholestane
D1	C1-Decalins	**FL0**	**Fluoranthene**	T5	C24 Tricyclic Terpane	S5	13b(H),17a(H)-20R-Diacholestane
D2	C2-Decalins	**PY0**	**Pyrene**	T6	C25 Tricyclic Terpane	S8	13b,17a-20S-Methyldiacholestane
D3	C3-Decalins	FP1	C1-Fluoranthenes/Pyrenes	T6a	C24 Tetracyclic Terpane	S12/S13	14a(H),17a(H)-20S-Cholestane +
D4	C4-Decalins	FP2	C2-Fluoranthenes/Pyrenes	T6b	C26 Tricyclic Terpane-22S		13b(H),17a(H)-20S-Ethyldiacholestane
BT0	Benzothiophene	FP3	C3-Fluoranthenes/Pyrenes	T6c	C26 Tricyclic Terpane-22R	S17/S18	14a(H),17a(H)-20R-Cholestane +
BT1	C1-Benzo(b)thiophenes	FP4	C4-Fluoranthenes/Pyrenes	T7	C28 Tricyclic Terpane-22S		13b(H),17a(H)-20R-Ethyldiacholestane
BT2	C2-Benzo(b)thiophenes	NBT0	Naphthobenzothiophenes	T8	C28 Tricyclic Terpane-22R	S18x	Unknown sterane
BT3	C3-Benzo(b)thiophenes	NBT1	C1-Naphthobenzothiophenes	T9	C29 Tricyclic Terpane-22S	S19	13a,17b-20S-Ethyldiacholestane
BT4	C4-Benzo(b)thiophenes	NBT2	C2-Naphthobenzothiophenes	T10	C29 Tricyclic Terpane-22R	S20	14a,17a-20S-Methylcholestane
N0	**Naphthalene**	NBT3	C3-Naphthobenzothiophenes	T11	18a-22,29,30-Trisnorneohopane-TS	S24	14a,17a-20R-Methylcholestane
N1	C1-Naphthalenes	NBT4	C4-Naphthobenzothiophenes	T11a	C30 Tricyclic Terpane-22S	S25	14a(H),17a(H)-20S-Ethylcholestane
N2	C2-Naphthalenes	**BA0**	**Benz[a]anthracene**	T11b	C30 Tricyclic Terpane-22R	S28	14a(H),17a(H)-20R-Ethylcholestane
N3	C3 Naphthalenes	**C0**	**Chrysene/Triphenylene**	T12	17a(H) 22,29,30 Trisnorhopane TM	S14	14b(H),17b(H) 20R Cholestane
N4	C4-Naphthalenes	BC1	C1-Chrysenes	T14a	17a/b,21b/a 28,30-Bisnorhopane	S15	14b(H),17b(H)-20S-Cholestane
B	Biphenyl	BC2	C2-Chrysenes	T14b	17a(H),21b(H)-25-Norhopane	S22	14b,17b-20R-Methylcholestane
DF	Dibenzofuran	BC3	C3-Chrysenes	T15	30-Norhopane	S23	14b,17b-20S-Methylcholestane
AY	**Acenaphthylene**	BC4	C4-Chrysenes	T16	18a(H)-30-Norneohopane-C29Ts	S26	14b(H),17b(H)-20R-Ethylcholestane
AE	**Acenaphthene**	BBF	Benzo[b]fluoranthene	X	17a(H)-Diahopane	S27	14b(H),17b(H)-20S-Ethylcholestane
F0	**Fluorene**	**BJKF**	**Benzo[jk]fluoranthene**	T17	30-Normoretane	RC26/SC27TA	C26,20R- +C27,20S- triaromatic steroid
F1	C1-Fluorenes	**BAF**	**Benzo[a]fluoranthene**	T18	18a(H)&18b(H)-Oleananes	SC28TA	C28,20S-triaromatic steroid
F2	C2-Fluorenes	BEP	Benzo[e]pyrene	T19	Hopane	RC27TA	C27,20R-triaromatic steroid
F3	C3-Fluorenes	**BAP**	**Benzo[a]pyrene**	T20	Moretane	RC28TA	C28,20R-triaromatic steroid
A0	**Anthracene**	PER	Perylene	T21	30-Homohopane-22S		
P0	**Phenanthrene**	**IND**	**Indeno[1,2,3-cd]pyrene**	T22	30-Homohopane-22R		
PA1	C1-Phenanthrenes/Anthracenes	**DA**	**Dibenz[a,h]anthracene**	T26	30,31-Bishomohopane-22S		
PA2	C2-Phenanthrenes/Anthracenes	**GHI**	**Benzo[g,h,i]perylene**	T27	30,31-Bishomohopane-22R		
PA3	C3-Phenanthrenes/Anthracenes			T30	30,31-Trishomohopane-22S		
PA4	C4-Phenanthrenes/Anthracenes	TPAH50	Σ N0 through GHI, excl PER	T31	30,31-Trishomohopane-22R		
DBT0	Dibenzothiophene	TPAH16	Σ bold compounds	T32	Tetrakishomohopane-22S		
DBT1	C1-Dibenzothiophenes			T33	Tetrakishomohopane-22R		
DBT2	C2-Dibenzothiophenes			T34	Pentakishomohopane-22S		
DBT3	C3-Dibenzothiophenes			T35	Pentakishomohopane-22R		
DBT4	C4-Dibenzothiophenes						

Table 3: Concentrations of hydrocarbons in sediment trap samples.

		HYDROCARBON CONCENTRATIONS (µg/g dry)				
Sample	Mid-Date	TPH	TPAH16	TPAH50	Hopane	Perylene
Cup 1	4-Sep-10	625	0.339	1.637	0.176	0.042
Cup 2	25-Sep-10	422	0.074	0.791	0.165	0.016
Cup 3	16-Oct-10	383	0.088	0.803	0.167	0.022
Cup 4	6-Nov-10	431	0.100	0.970	0.223	0.019
Cup 5	27-Nov-10	559	0.126	1.358	0.242	0.021
Cup 6	18-Dec-10	474	0.132	1.801	0.275	0.021
Cup 7	8-Jan-11	352	0.093	0.840	0.149	0.017
Cup 8	29-Jan-11	318	0.092	0.796	0.137	0.015
Cup 9	19-Feb-11	217 J	0.082	0.719	0.113	0.017
Cup 10	12-Mar-11	253	0.104	0.817	0.100	0.038
Cup 11	2-Apr-11	308	0.097	0.982	0.122	0.027
Cup 12	23-Apr-11	172	0.107	0.859	0.108	0.020
Cup 13	14-May-11	182 J	0.092	0.663	0.103	0.019
Cup 14	4-Jun-11	137 J	0.094	0.545	0.079	0.022
Cup 15	25-Jun-11	155 J	0.094	0.616	0.105	0.019
Cup 16	16-Jul-11	118 J	0.083	0.418	0.074	0.017
Cup 17	6-Aug-11	105 J	0.070	0.310	0.067	0.011
Cup 18	27-Aug-11	123 J	0.066	0.286	0.079	0.014
Cup 19	17-Sep-11	211	0.048	0.064	0.045	0.017
J - concentration is estimated; below RL						

Table 4: Sedimentation rates of hydrocarbons (left) and bulk metrics (PIM, POM, POC, lithogenic and biogenic silica) in sediment trap samples.

		HYDROCARBON SEDIMENTATION RATES ($\mu g/m^2/day$)				BULK SEDIMENTATION RATES ($mg/m^2/day$)			
Sample	Mid-Date	TPH	TPAH16	TPAH50	Hopane	PIM	POM	Litho-Silica	Bio-Silica
Cup 1	4-Sep-10	1146	0.62	3.00	0.32	1228	334	802	397
Cup 2	25-Sep-10	287	0.05	0.54	0.11	469	198	345	117
Cup 3	16-Oct-10	204	0.05	0.43	0.09	334	89	283	44
Cup 4	6-Nov-10	240	0.06	0.54	0.12	402	101	337	57
Cup 5	27-Nov-10	149	0.03	0.36	0.06	208	53	177	22
Cup 6	18-Dec-10	296	0.08	1.12	0.17	513	156	451	47
Cup 7	8-Jan-11	182	0.05	0.43	0.08	348	115	286	48
Cup 8	29-Jan-11	133	0.04	0.33	0.06	288	137	234	39
Cup 9	19-Feb-11	104	0.04	0.35	0.05	234	87	194	30
Cup 10	12-Mar-11	388	0.16	1.25	0.15	998	265	853	119
Cup 11	2-Apr-11	243	0.08	0.77	0.10	558	168	491	51
Cup 12	23-Apr-11	136	0.08	0.68	0.09	582	172	494	76
Cup 13	14-May-11	72	0.04	0.26	0.04	177	66	151	22
Cup 14	4-Jun-11	75	0.05	0.30	0.04	542	196	455	71
Cup 15	25-Jun-11	75	0.05	0.30	0.05	369	84	310	51
Cup 16	16-Jul-11	46	0.03	0.16	0.03	204	87	167	32
Cup 17	6-Aug-11	41	0.03	0.12	0.03	305	119	238	59
Cup 18	27-Aug-11	56	0.03	0.13	0.04	212	79	161	44
Cup 19	17-Sep-11	142	0.03	0.04	0.03	265	132	184	77

Table 5: Hopane-based mass and volume of Macondo oil deposited on the seafloor in the area and time period represented by the sediment trap.

HOPANE-BASED MACONDO OIL SEDIMENTATION RATE								
Sample	Mid-Date	Hopane Flux (mg/m^2/ day)	Mass Oil* (kg/km^2/ day)	Volume Oil** (bbl/km^2/ day)	Mass Oil (kg/km^2 per 21-day sampling interval)	Volume Oil (bbl/km^2 per 21-day sampling interval)	Cumulative Percent of Total (Cups 1 to 18)	
Cup 1	4-Sep-10	3.23E-04	4.69	0.034	98.5	0.72	20	Pulse 1
Cup 2	25-Sep-10	1.12E-04	1.63	0.012	34.3	0.25	7	
Cup 3	16-Oct-10	8.90E-05	1.29	0.010	27.2	0.20	5	
Cup 4	6-Nov-10	1.24E-04	1.80	0.013	37.8	0.28	8	
Cup 5	27-Nov-10	6.44E-05	0.94	0.007	19.7	0.14	4	
Cup 6	18-Dec-10	1.71E-04	2.49	0.018	52.3	0.38	10	Pulse 2
Cup 7	8-Jan-11	7.72E-05	1.12	0.008	23.6	0.17	5	
Cup 8	29-Jan-11	5.77E-05	0.84	0.006	17.6	0.13	4	
Cup 9	19-Feb-11	5.44E-05	0.79	0.006	16.6	0.12	3	
Cup 10	12-Mar-11	1.53E-04	2.22	0.016	46.6	0.34	9	
Cup 11	2-Apr-11	9.62E-05	1.40	0.010	29.4	0.22	6	Pulse 3
Cup 12	23-Apr-11	8.56E-05	1.24	0.009	26.1	0.19	5	
Cup 13	14-May-11	4.06E-05	0.59	0.004	12.4	0.09	2	
Cup 14	4-Jun-11	4.29E-05	0.62	0.005	13.1	0.10	3	
Cup 15	25-Jun-11	5.12E-05	0.74	0.005	15.6	0.11	3	Pulse 4
Cup 16	16-Jul-11	2.91E-05	0.42	0.003	8.9	0.07	2	
Cup 17	6-Aug-11	2.60E-05	0.38	0.003	7.9	0.06	2	
Cup 18	27-Aug-11	3.59E-05	0.52	0.004	10.9	0.08	2	

* hopane in fresh oil 68.8 mg/kg

** density 0.8560 g/cm^3 at 5°C; bbl = barrels (42 US gallons)

	Cumulative Totals (kg)	Cumulative Totals (bbl)
Totals (Cups 1 to 12):	430	3.2
Totals (Cups 1 to 18):	499	3.7

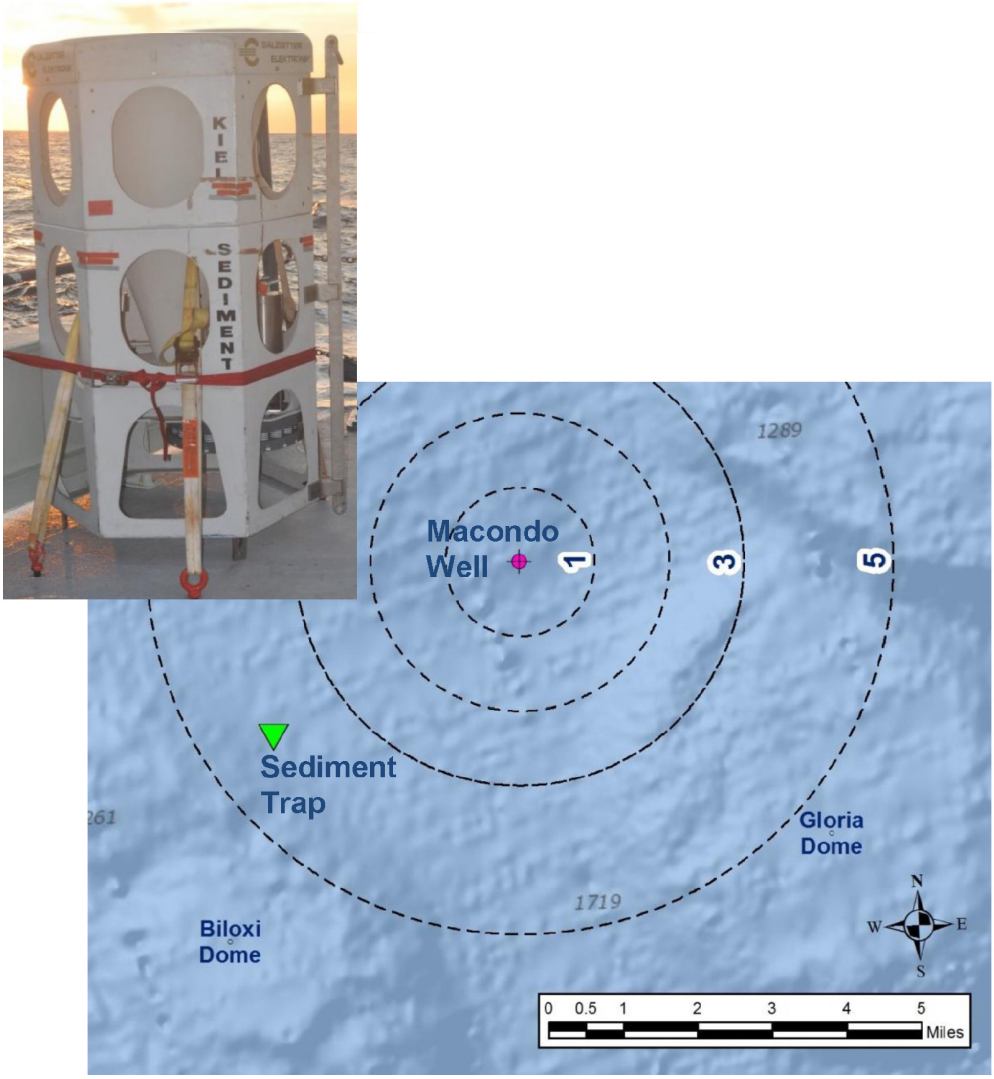

Figure 1: Map showing the location of the sediment trap relative to the Macondo well and Biloxi Dome. Concentric rings in miles. Photograph (by author Uta Passow) shows funnel-shaped Kiel; note sample bottle carousel visible at the bottom of the trap.

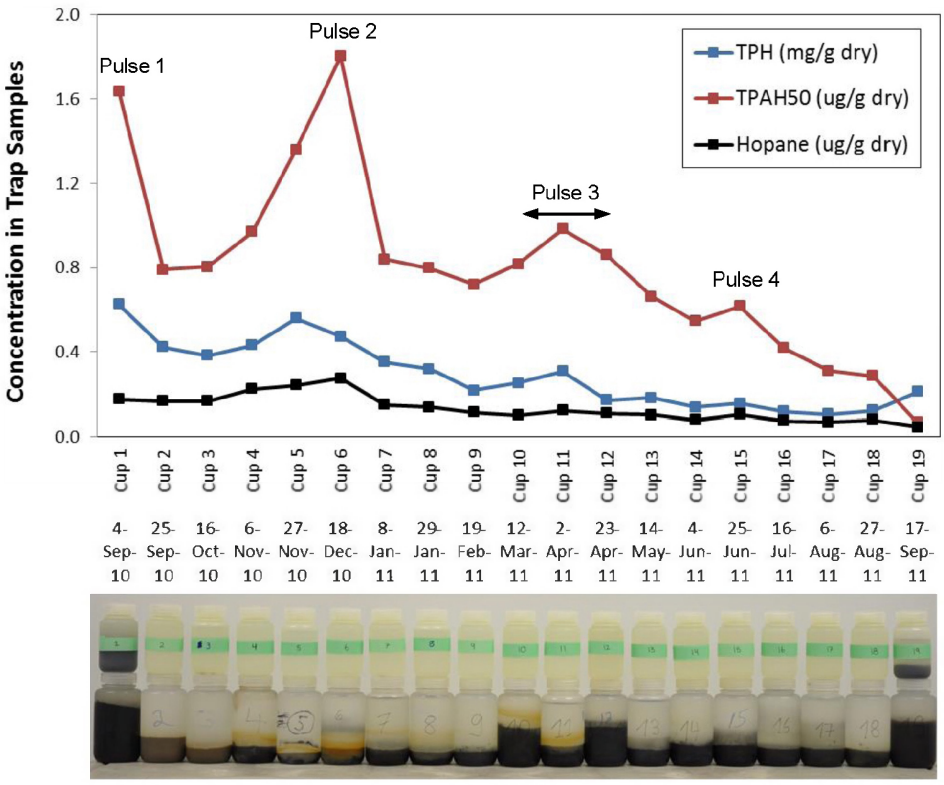

Figure 2: Plot showing the concentrations of hydrocarbons in sediment trap samples collected over time. All data from Table 3. Note the different units. Photograph at bottom shows the original sample bottle appearance.

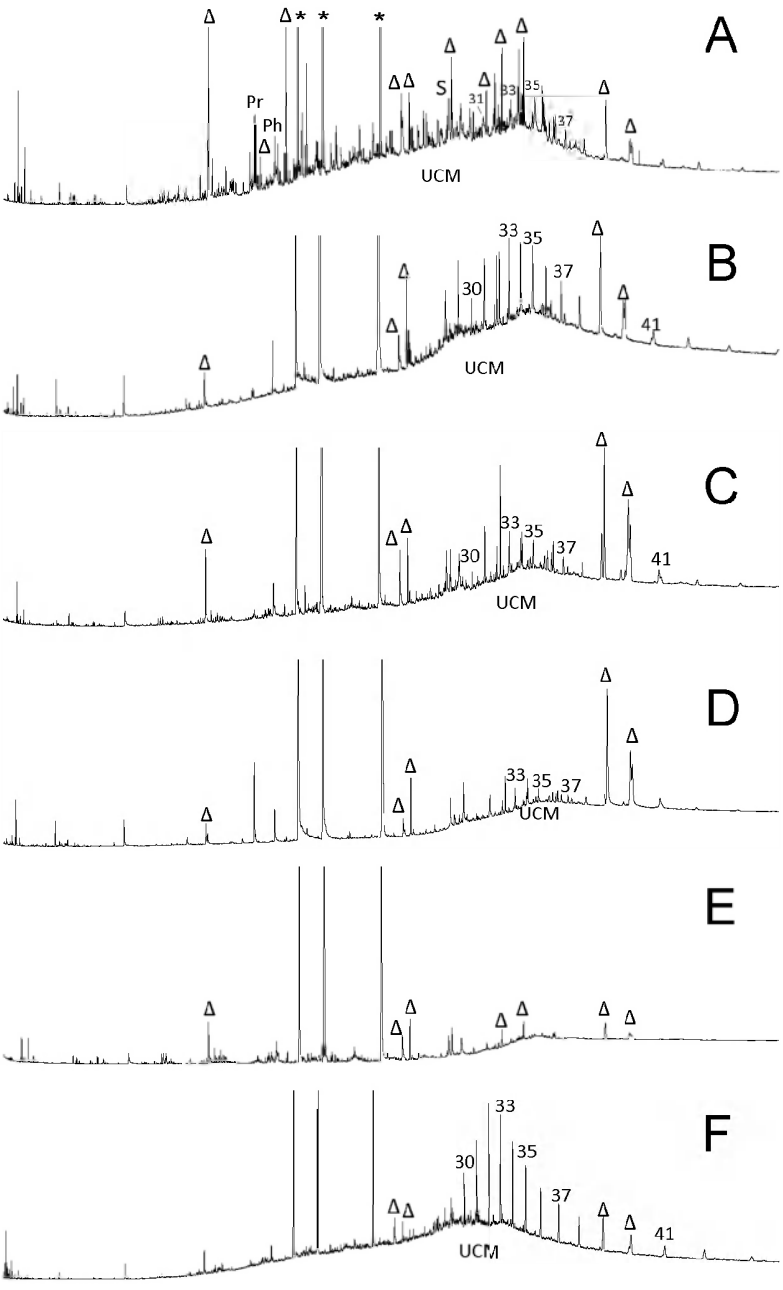

Figure 3: GC/FID chromatograms for TPH in (A) Cup 1 (Pulse 1; Aug 2010), (B) Cup 6 (Pulse 2; Dec. 2010), (C) Cup 11 (Pulse 3; April 2011), (D) Cup 15 (Pulse 4; June 2011), (E) Cup 19 (Sept. 2011) and (F) typical seafloor floc in surface sediment (0-1 cm; SB9-65-B0528-S-LBNL3-HC-0929) collected in May 2011 about 1 km southeast of the trap. * - internal standards; S – squalene; Δ - unidentified unsaturated branched isoprenoids and cyclic terpenoids attributed to biomass (not oil); # - n-alkane carbon number; UCM – unresolved complex mixture.

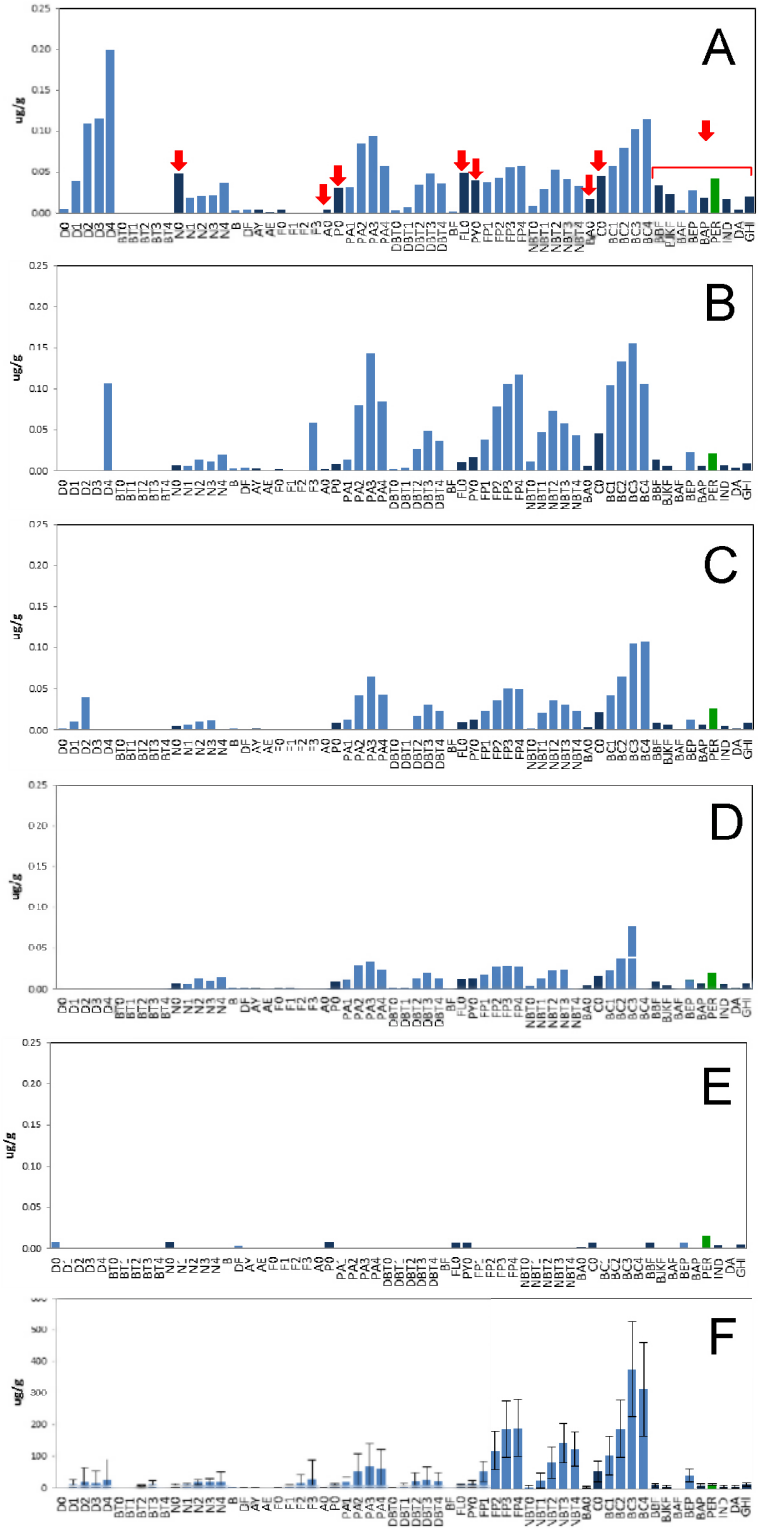

Figure 4: Histograms showing concentrations of PAHs in (A) Cup 1 (Pulse 1; Aug 2010), (B) Cup 6 (Pulse 2; Dec. 2010), (C) Cup 11 (Pulse 3; Mar. 2011), (D) Cup 15 (Pulse 4; June 2011), (E) Cup 19 (Sept. 2011) and (F) average seafloor floc containing Macondo oil in surface (0-1 cm) sediments collected 3 to 5 miles from the wellhead (n=20; from Stout, 2015, in preparation). All concentrations in μg/g dry wt. For compound abbreviations see Table 2. Dark blue bars indicate Priority Pollutant PAH used in calculating TPAH16. Green bar is perylene attributed largely to biomass, not oil. Arrows indicate excess Priority Pollutant PAHs; see text for description. Error bars in (E) = 1σ.

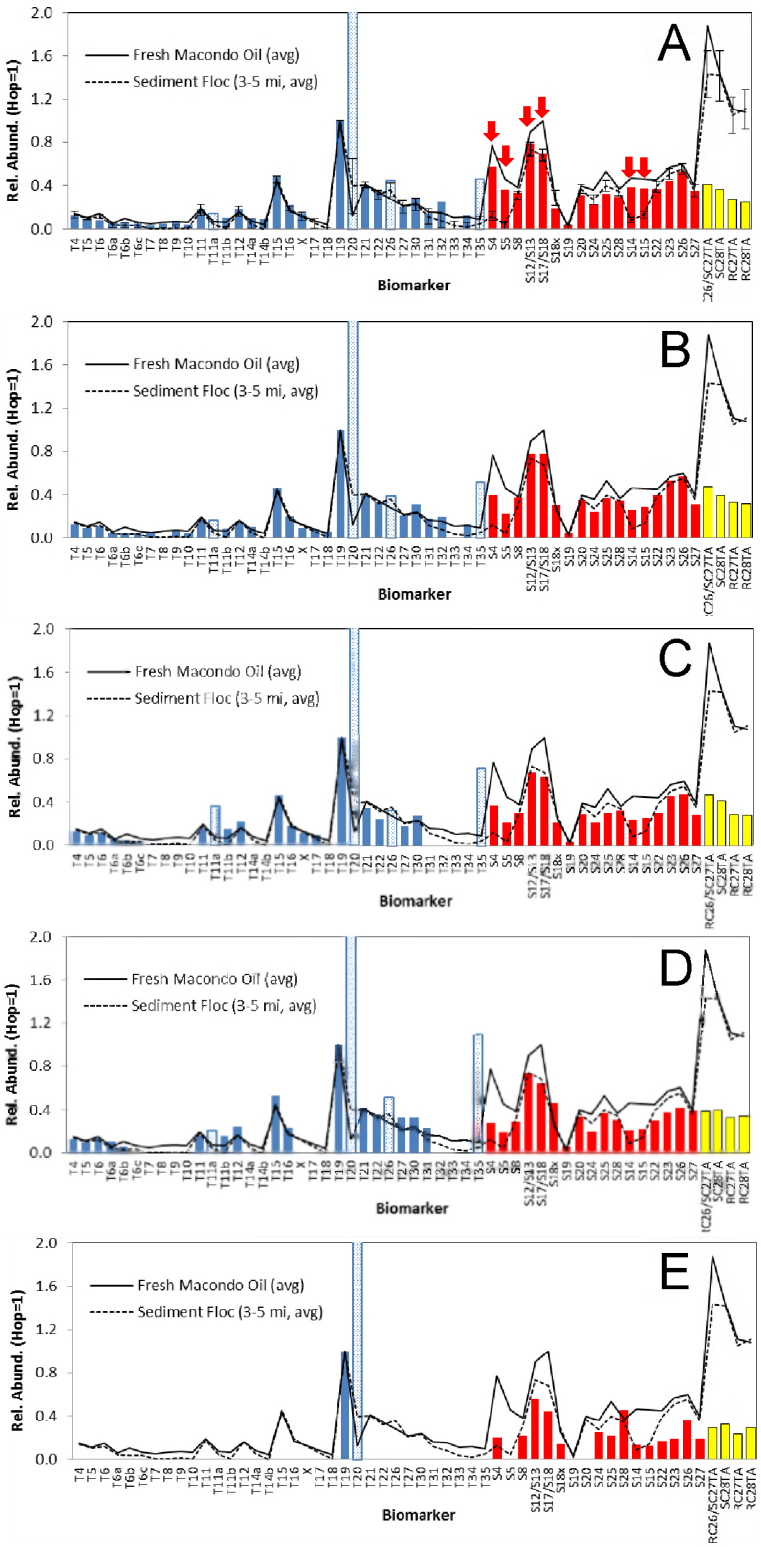

Figure 5: Histograms showing hopane-normalized distributions of triterpanes (blue), steranes and diasteranes (red), and triaromatic steroids (yellow) in (A) Cup 1 (Pulse 1; Aug 2010), (B) Cup 6 (Pulse 2; Dec. 2010), (C) Cup 11 (Pulse 3; Mar. 2011), (D) Cup 15 (Pulse 4; June 2011) and (E) Cup 19 (Sept. 2011). Light blue stipple indicates naturally-occurring interferences with target analytes. Distributions for fresh Macondo oil (Stout, 2014a) and average seafloor floc containing Macondo oil in surface (0-1 cm) sediments 3 to 5 miles from the wellhead (per Stout, 2015, in preparation) are given for comparison. Arrows indicate biodegradation susceptible C_{27} βα-diasteranes (S4 and S5) and C_{27} ββ-steranes (S14 & S15); loss of C_{27} αα-steranes (S12 and S17) is suspected but confounded by co-elutions; see text. Error bars in (A) = 1σ.

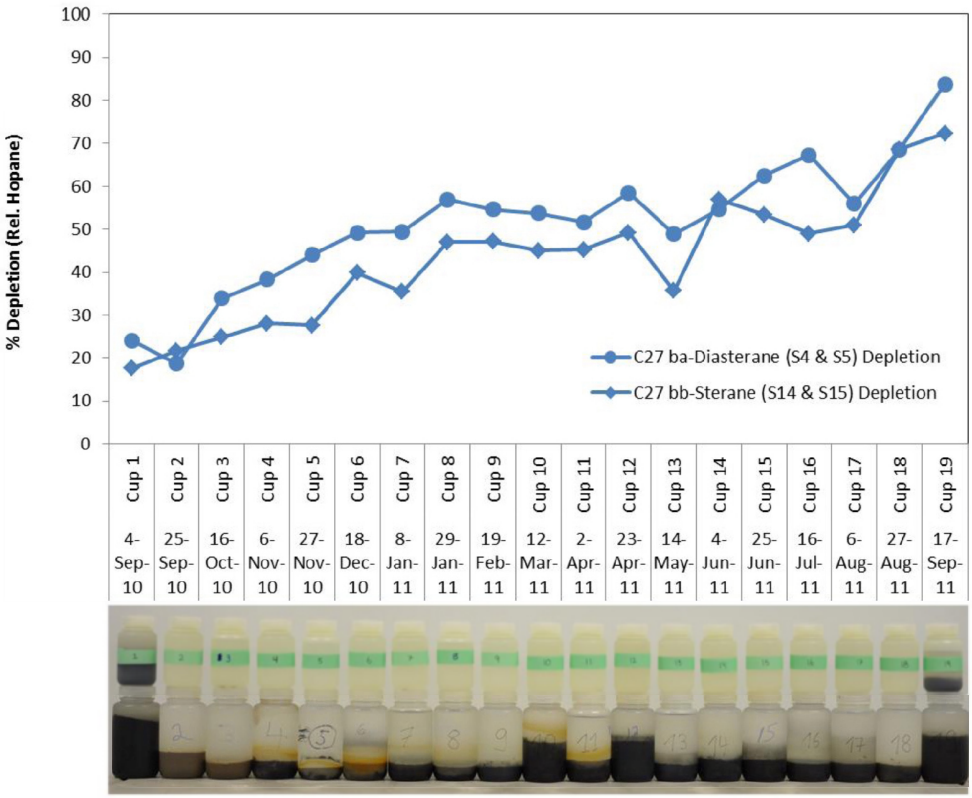

Figure 6: Plot showing percent depletions (relative to hopane; Eq. 1) of C_{27} βα-diasteranes and C_{27} ββ-steranes in sediment trap samples collected over time. Increased depletion over time shows progressive biodegradation of these biomarkers occurred in the water column. Photograph at bottom shows the original sample bottle appearance.

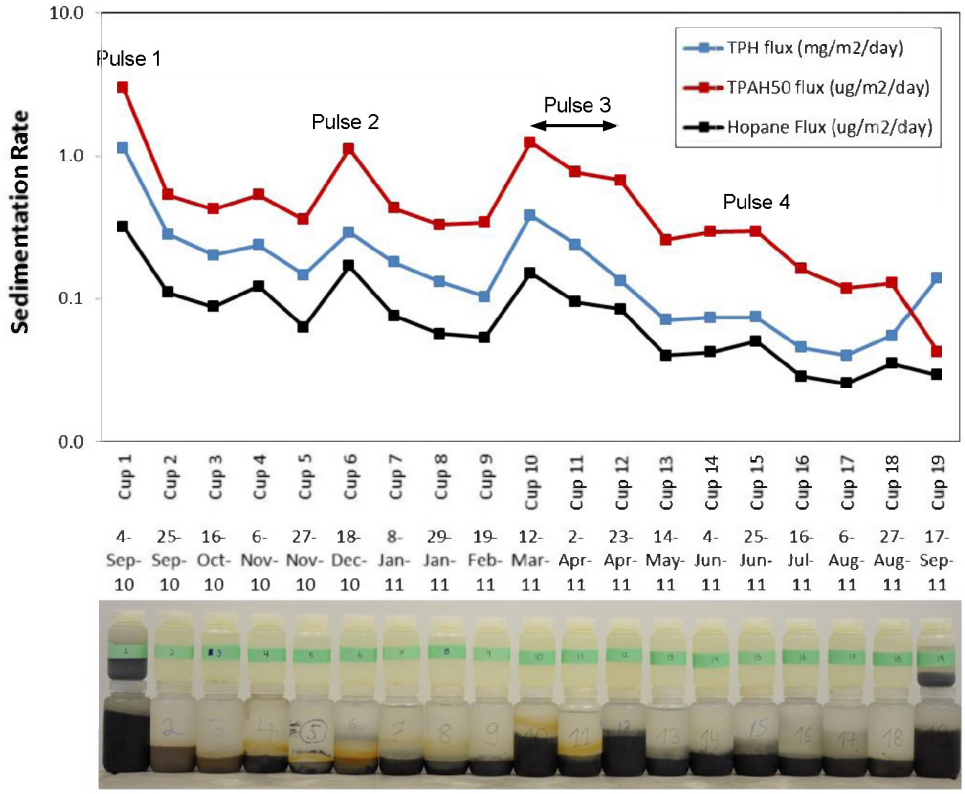

Figure 7: Plot showing flux of hydrocarbons in sediment trap samples collected over time. All data from Table 4. Note the units for TPH are different than for TPAH50 and hopane. Photograph at bottom shows the original sample bottle appearance.

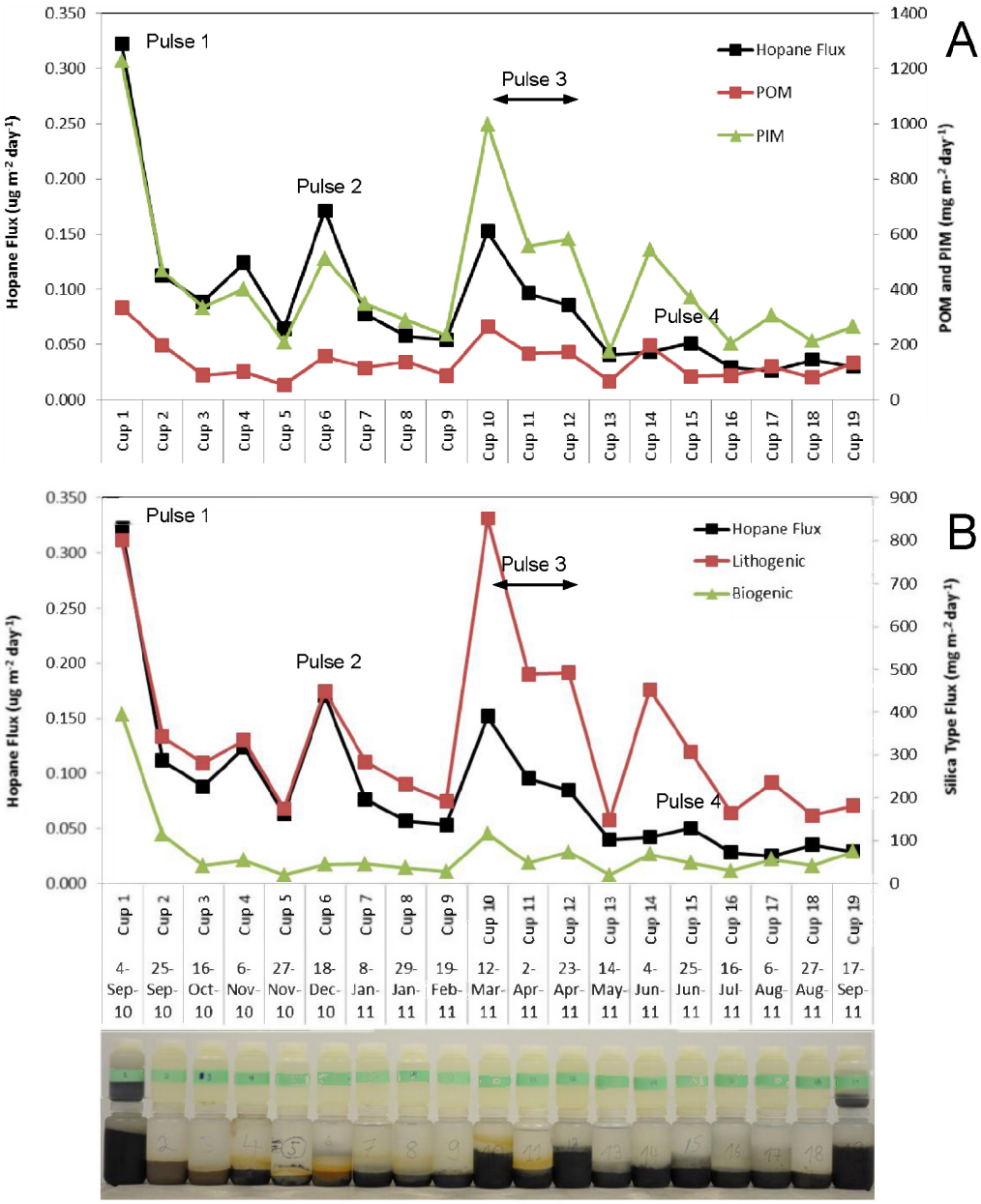

Figure 8: Plots showing fluxes of hopane versus (A) POM and PIM and (B) silica type (lithogenic and biogenic) in sediment trap samples collected over time. All data from Table 4. Photograph at bottom shows the original sample bottle appearance.

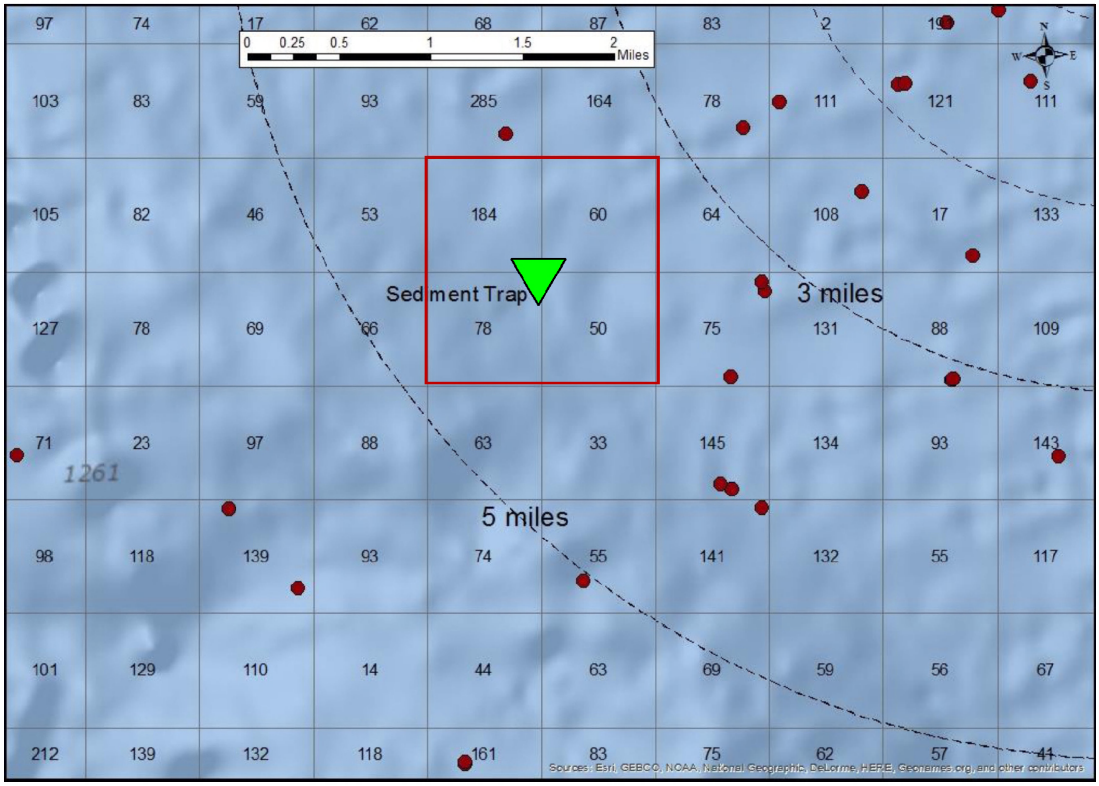

Figure 9: Map showing the location of the sediment trap studied and the average Macondo-derived (i.e., non-background) hopane concentrations in km^2 blocks located two to six miles southwest of the wellhead (as per Stout et al. 2015). These concentrations reflect the average "excess" (non-background) hopane contained in Macondo-derived seafloor floc found in surface sediments (0-1 cm) about 2 to 6 miles southwest of the wellhead. Red points show the locations of cores containing Macondo-derived seafloor floc from which "excess" average hopane concentrations were calculated and interpolated. The four km^2 around the sediment trap (red square) have an average ($\pm$ σ) "excess" hopane concentration of 93 $\pm$ 62 μg/kg.